

Received 21 September 2023

Accepted 29 November 2023

Edited by N. Alvarez Failache, Universidad de la
República, Uruguay**Keywords:** dicopper; carboxylate; pyrene; $\pi-\pi$
stacking; crystal structure.**CCDC reference:** 2281680**Supporting information:** this article has
supporting information at journals.iucr.org/e

New copper carboxylate pyrene dimers: synthesis, crystal structure, Hirshfeld surface analysis and electrochemical characterization

Vianca C. Nogué-Guzmán,^a Alejandro Burgos-Suazo,^b Javier O. Rivera-Reyes,^b
Vasti P. Montes Quiñones,^a Paola C. Ramis-Aybar,^a Adriana C. Burgos-Jiménez,^a
Karilys González-Nieves^{a*} and Dalice M. Piñero-Cruz^{b,c*}

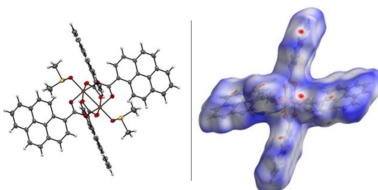
^aDepartment of Natural Sciences, University of Puerto Rico, Carolina Campus, Carolina, 00984-4800, Puerto Rico,

^bDepartment of Chemistry, University of Puerto Rico, Rio Piedras Campus, San Juan, 00927, Puerto Rico, and ^cUniversity of Puerto Rico's Molecular Sciences Research Center, San Juan, 00926, Puerto Rico. *Correspondence e-mail:
karilys.gonzalez@upr.edu, dalice.pinero@upr.edu

Two new copper dimers, namely, bis(dimethyl sulfoxide)tetrakis(μ -pyrene-1-carboxylato)dicopper(Cu–Cu), $[\text{Cu}_2(\text{C}_{17}\text{H}_9\text{O}_2)_4(\text{C}_2\text{H}_6\text{OS})_2]$ or $[\text{Cu}_2(\text{pyr-COO}^-)_4(\text{DMSO})_2]$ (**1**), and bis(dimethylformamide)tetrakis(μ -pyrene-1-carboxylato)dicopper(Cu–Cu), $[\text{Cu}_2(\text{C}_{17}\text{H}_9\text{O}_2)_4(\text{C}_3\text{H}_7\text{NO})_2]$ or $[\text{Cu}_2(\text{pyr-COO}^-)_4(\text{DMF})_2]$ (**2**) (pyr = pyrene), were synthesized from the reaction of pyrene-1-carboxylic acid, copper(II) nitrate and triethylamine from solvents DMSO and DMF, respectively. While **1** crystallized in the space group $P\bar{1}$, the crystal structure of **2** is in space group $P2_1/n$. The Cu atoms have octahedral geometries, with four oxygen atoms from carboxylate pyrene ligands occupying the equatorial positions, a solvent molecule coordinating at one of the axial positions, and a Cu··Cu contact in the opposite position. The packing in the crystal structures exhibits $\pi-\pi$ stacking interactions and short contacts through the solvent molecules. The Hirshfeld surfaces and two-dimensional fingerprint plots were generated for both compounds to better understand the intermolecular interactions and the contribution of heteroatoms from the solvent ligands to the crystal packing. In addition, a $\text{Cu}^{2+}/\text{Cu}^{1+}$ quasi-reversible redox process was identified for compound **2** using cyclic voltammetry that accounts for a diffusion-controlled electron-donation process to the Cu dimer.

1. Chemical context

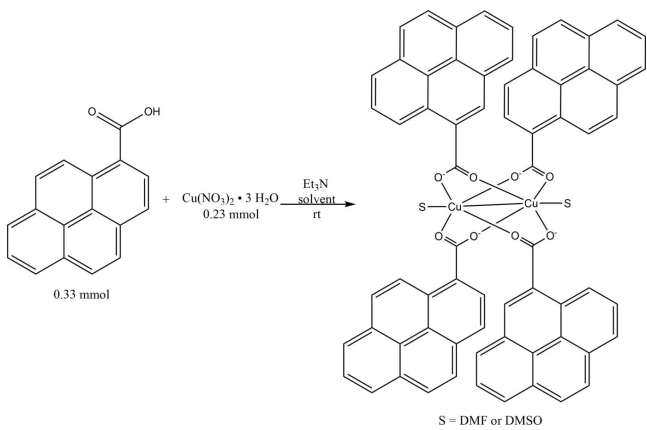
Copper(II) carboxylate complexes with paddle-like structure have been proposed in solar energy conversion and storage, redox mediators, magnetism, dyes and in catalysis, among other applications (Benesperi *et al.* 2020; Kozlevčar *et al.*, 2004; Rajakannu *et al.*, 2019; Murugavel *et al.*, 2000; Rao *et al.*, 2004; Boulourani *et al.*, 2017; Baldomá *et al.*, 2006; Seo *et al.*, 2000). The unique characteristics of copper(II) carboxylate complexes of general formula $[\text{Cu}_2(\text{RCOO}^-)_4(L)_2]$ are based on their easy synthesis, the relative abundance of the starting materials, their stability, and their low toxicity, which enables a vast number of research directions to be performed from such materials. The structural features of these compounds are related to the coordinating aspect of the ligands: the two possible coordination sites through the carboxylate oxygen atoms result in various modes of coordination, such as monodentate, bidentate and bridging, offering a variability of polynuclear metal complexes (Rajakannu *et al.*, 2019; Murugavel *et al.*, 2000; Rao *et al.*, 2004), and a degree of stability for dinuclear and trinuclear complexes. Additionally, the carboxylate group could participate in hydrogen bonds,



OPEN ACCESS

Published under a CC BY 4.0 licence

leading to a supramolecular network (Aakeröy *et al.*, 2006). Moreover, dinuclear copper(II) carboxylate complexes may have switchable electronic properties such as intermetal magnetic exchange and electron transfer (Vishnoi *et al.*, 2017). The electrochemical properties of copper(II) carboxylate complexes are reported to be highly influenced by the redox-active nature of copper(II/I) and subjected to potential changes due to the presence of substituents in the carboxylate ligands (Wang *et al.*, 2013), thereby influencing the stability of its oxidation state (Modec *et al.*, 2020).



In this work we report the structure of two new copper(II) carboxylate complexes from pyrene-1-carboxylic acid. The structure of pyrene is based on four fused benzene rings, thus it belongs to the group of polycyclic aromatic hydrocarbons (PAH) that have been well studied since their remarkable fluorescence and phosphorescence properties were noted (Halder *et al.*, 2020). Carboxylic acid from 1-pyrene has been proposed in supercapacitor devices by functionalization of graphene and it is also used to design and synthesize luminescent metal–organic complexes for sensing applications.

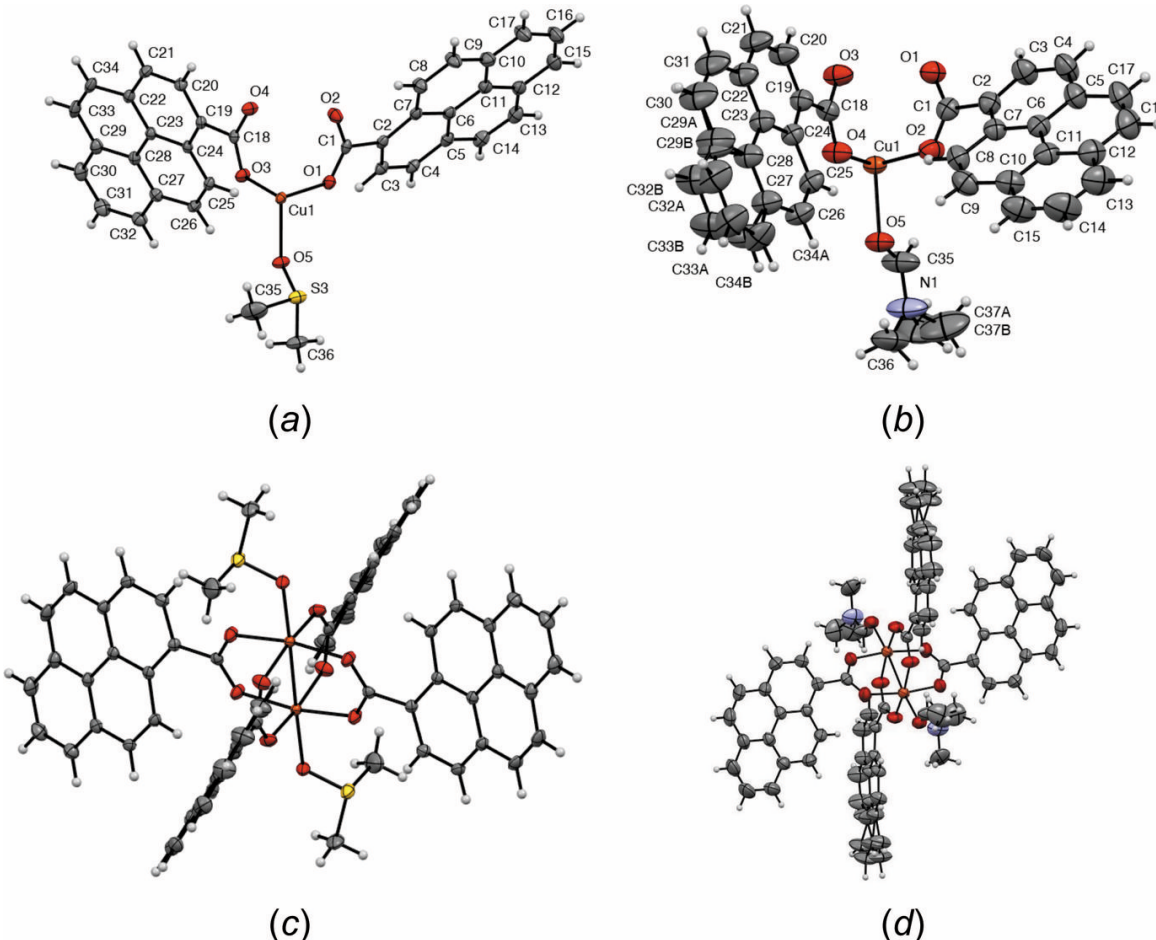
In addition, pyrene ligands have been used as an organic linker or as building blocks for the design of new classes of metal–organic frameworks (MOFs). The functionalization of pyrene with phosphonates, sulfonates, and carboxylates allows metal coordination to yield MOF structures exhibiting new photophysical and photochemical properties. MOF structures with pyrene ligands result in promising optical properties such as luminescence sensing, photocatalysis, electrochemistry, adsorption and separation applications, and biomedical applications (Kinik *et al.*, 2021). Derivatives of carboxylate pyrene ligands have been studied because of their extraordinary photophysical properties, chemical stability, π – π stacking interactions, and high-charge-delocalized systems (Guan *et al.*, 2019). The planar π -conjugated surface of pyrene and its molecular rearrangement is favorable for the detection of guest molecules in molecular tweezer hosts, for example with platinum, ruthenium, and copper complexes. Another application of pyrene can be found in the functionalization of carbon nanotubes (CNTs) as a result of its π – π interactions with polycyclic aromatic molecules (Zhao & Stoddart, 2009).

Here, we report the novel synthesis, characterization, and crystal structure of two copper dimers with tetracarboxylate

pyrene and two solvent molecules in axial positions, $[\text{Cu}_2(\text{pyr-COO}^-)_4(\text{DMSO})_2]$ (**1**) and $[\text{Cu}_2(\text{pyr-COO}^-)_4(\text{DMF})_2]$ (**2**). Structural characterization from single-crystal X-ray diffraction experiments show crystallization under two crystal systems, which translates into different extended contacts, such as π – π stacking interactions, among others. In terms of the chemistry of these copper structures, they are very promising because the axial positions can be substituted by bridging ligands, which can form coordination polymers such as the 1D, 2D, and 3D polymeric architectures that have been proposed in molecular sensing, gas storage, and separation (Karmakar *et al.*, 2021). Hirshfeld surface analysis was undertaken to show the contributions from intermolecular interactions in the crystal-packing array. The pyrene rings participate in π – π interactions, yet some rings have weaker interactions based on their position in the crystal structure. DMSO (**1**) and DMF (**2**) axial ligands, play a crucial role in the crystal packing by participating in interactions with the rest of the molecule. In addition, Hirshfeld surface analysis showed that compound **2** has shorter distances for most interactions. Electrochemical characterization of compound **2** was performed by cyclic voltammetry at varying scan rates (50–2000 mV s^{−1}), revealing a diffusion-controlled $\text{Cu}^{2+}/\text{Cu}^{1+}$ quasi-reversible process that may involve an electron reduction at an $E_{1/2}$ potential around −0.52 V vs F_c/F_c^+ (Iqbal *et al.*, 2013; Bonomo *et al.*, 2000).

2. Structural commentary

The crystal structures of complexes $[\text{Cu}_2(\text{pyr-COO}^-)_4(\text{DMSO})_2]$ (**1**), space group $P\bar{1}$, and $[\text{Cu}_2(\text{pyr-COO}^-)_4(\text{DMF})_2]$, space group $P2_1/n$ (**2**), are presented in Fig. 1. The copper atoms have octahedral geometries with four oxygen atoms from the pyrene-1-carboxylate ligand at equatorial positions, one axial ligand from the solvent molecule and the remaining axial coordination occupied by a metal–metal copper contact. The asymmetric unit contains half the molecule in both structures. The $\text{Cu}\cdots\text{Cu}$ contact distance in **1** is 2.5934 (3) Å in comparison with the structure of **2** for which it is 2.6295 (5) Å. Likewise, the $\text{Cu}–\text{O}5$ bond distance in the axial position is shorter in **1** than in **2**, with values of 2.1441 (12) and 2.1769 (13) Å, respectively. The difference in the elongation of these bond distances could be the result of the influence of the axial ligand (DMSO vs DMF) with stronger π -back-bonding character, thus better binding (Deacon & Phillips, 1980). The $\text{Cu}–\text{O}$ bonds in equatorial positions are shorter than those in axial positions in both structures, with distances ranging from 1.9530 (13) to 1.9593 (13) Å, which may be indicative of Jahn–Teller effects on Cu^{II} centers. All the other structural features in the two Cu dimers do not change significantly. Structural disorder of four carbon atoms from the pyrene (C29–C32–C33–C34) unit is observed in complex **2** as well as in one of the carbon atoms from the DMF molecule, precisely on C37, for which atoms had to be modeled in two parts.

**Figure 1**

Asymmetric units of Cu complexes **1** (a) and **2** (b) with labels for non-C/H atoms and ellipsoids at the 50% probability level. (c) and (d) views of the complete molecules from the *b* axis.

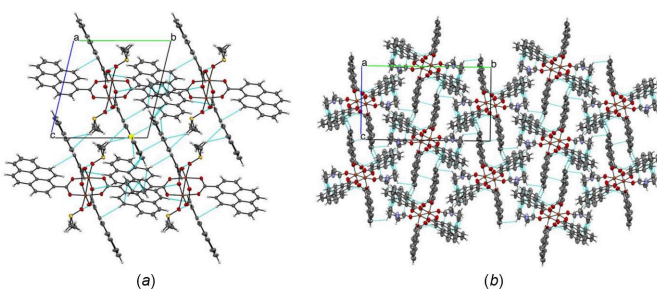
3. Supramolecular features

Long-range interactions for **1** and **2** are different in terms of their π - π stacking, as well as the axial hydrogen interactions with π rings. In the case of complex **1**, the most important π - π interactions is observed for C22···C16 at 3.393 (3) Å. C–H to π -ring interactions are observed between C28···H15 and C27···H15 at 2.87 and 2.90 Å, respectively, and the solvent oxygen interaction π -ring end hydrogen is observed through O5···H4 at a distance of 2.56 Å. In complex **2** however, π - π

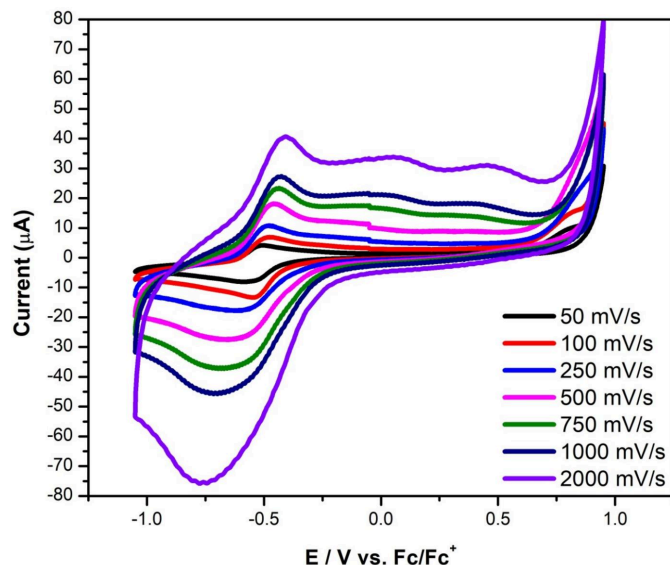
interactions are present from C4···C4 of neighboring rings with a distance 3.178 (4) Å; other interactions are attributed to C–H end to π -ring for C16···H37B, C19···H16, and C24···H16 with distances of 2.87, 2.85, and 2.70 Å, respectively. The packing for **1** and **2** is shown in Fig. 2.

4. Electrochemical measurements

Electrochemical properties were measured in DMF for complex **2**; complex **1** was not soluble therein, and thus was not characterized electrochemically. The cyclic voltammograms (CV) of compound **2** at multiple scan rates are shown in Fig. 3. The main feature presented by compound **2** exhibits a redox couple at *ca* −0.5 V vs F_c/F_c^+ associated with the Cu^{2+}/Cu^{1+} couple (Iqbal *et al.*, 2013; Bonomo *et al.*, 2000). This redox process was found to be quasi-reversible because as the scan rate increased, the peak-to-peak separation increased, indicating that this process is not reversible. Another indication of the quasi-reversible nature of compound **2** is that the ratio between the cathodic and anodic peak current is less than 1. According to the Randles–Sevcik equation, the observed linear relationship between the square root of the

**Figure 2**

Crystal packing of Cu complexes **1** and **2** along the *a* axis with ellipsoids at the 50% probability level.

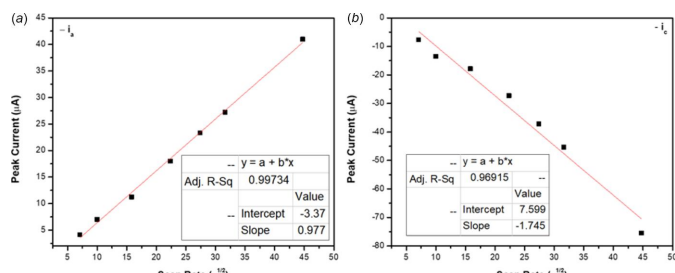
**Figure 3**

Cyclic voltammograms of 1 mM of compound **2** at $50\text{--}2000\text{ mV s}^{-1}$. Cyclic voltammograms were obtained in a 0.1 M TBAPF₆ in DMF with a glassy carbon working electrode, a graphite rod counter-electrode, and 0.01 M AgNO₃ silver wire as the pseudo-reference electrode corrected with ferrocene.

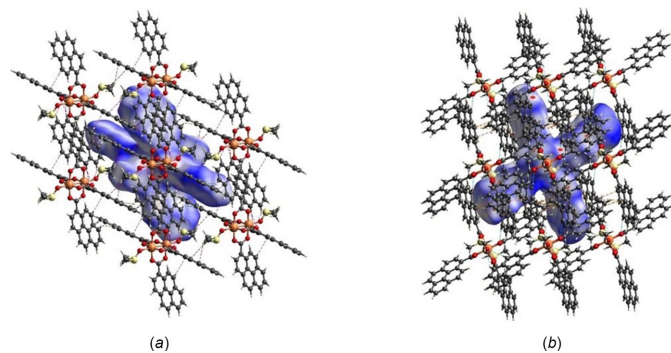
scan rate and the peak current confirms that the quasi-reversible process is diffusion-controlled (Fig. 4) (Elgrishi *et al.*, 2018). It was observed that on increasing the scan rates to 750 mV s^{-1} , two irreversible oxidation processes appeared at 0.05 and $0.50\text{ V vs } \text{F}_c/\text{F}_c^+$. In summary, complex **2** possesses a quasi-reversible diffusion-controlled redox process corresponding to the $\text{Cu}^{2+}/\text{Cu}^{1+}$ couple.

5. Hirshfeld surface analysis

The Hirshfeld surfaces were generated using *Crystal-Explorer17.5* software and evaluated over d_{norm} , shape-index, and curvedness. Fingerprint plot analysis was also carried out for **1** and **2** (Spackman *et al.*, 2021; Turner *et al.*, 2017; Spackman & Jayatilaka, 2009; Spackman & McKinnon, 2002). The Hirshfeld surface of **1** evaluated over d_{norm} shows multiple bright- and light-red spots (Figs. 5 and 6), revealing that many interactions take place and that the crystal packing is a compact one (*i.e.*, short distances). The red spots on the

**Figure 4**

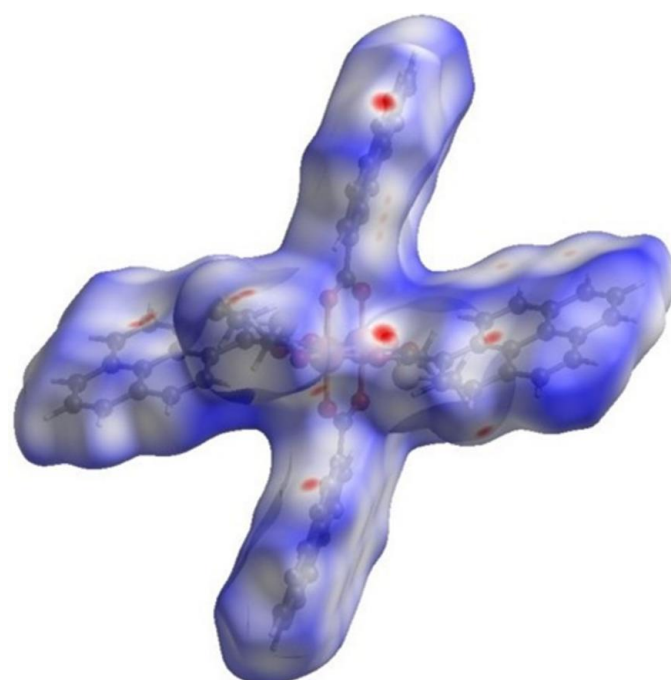
Square root of scan rate versus peak current plot (a) anodic peak and (b) cathodic peak of compound **2**.

**Figure 5**

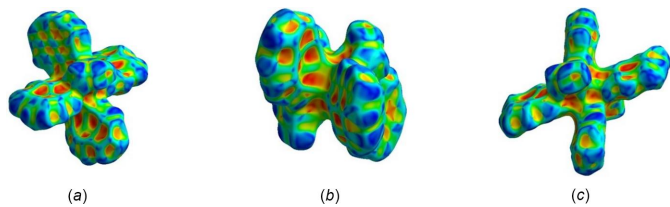
Hirshfeld surface evaluated over d_{norm} for title compound **1** with adjacent molecules showing short contacts (a) C···H/H···C (purple) and H···H (green), (b) H···O/O···H (blue) and C···C (orange).

surface, including the innermost region near the oxygen atoms (*e.g.*, O1···H34 at 2.53 \AA), equatorial pyrene moieties (core and edges, *e.g.*, C28···H15 at 2.87 \AA , H32···H9 at 2.38 \AA), and axial ligand positions (*e.g.*, O5···H4 at 2.56 \AA , H36B···C11 at 2.77 \AA), are mostly C···C, H···H, H···O/O···H, and C···H/H···C interactions (Fig. 5). The red spots on the surface region of axial ligands indicate that interactions with DMSO are a crucial component for the crystal packing.

Short interactions are better perceived in Fig. 6, both on the pyrene moiety (core and edges) and ligand positions. The role of pyrene rings in the crystal packing is evident, as well as for solvent molecules, even though their contributions are different (Fig. 7). Important π – π interactions are observed in the shape-index surface, represented by characteristic adjacent red-yellow and blue-green triangles (and back-to-back diamonds) on pyrene rings (Fig. 7a) and in the axial ligand

**Figure 6**

Hirshfeld surface evaluated over d_{norm} for title compound **1**.

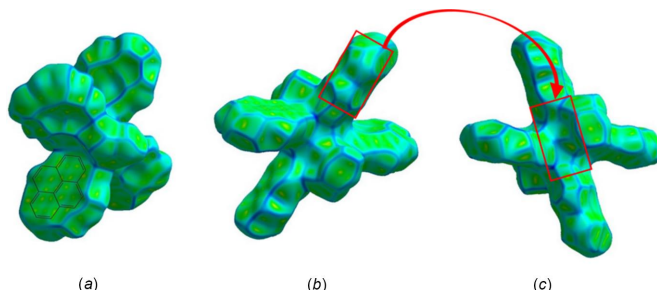
**Figure 7**

Hirshfeld surface evaluated over shape-index for title compound **1**, viewed from the side (*a*), (*b*) and top (*c*).

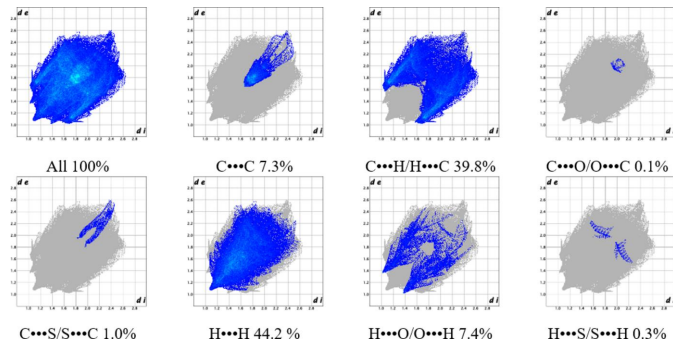
region (Fig. 7*c*). Interestingly, not all pyrene cores have the same degree of interactions within the crystal packing. The pyrene rings are either engaged in strong $\pi\cdots\pi$ interactions or in other interactions, predominantly of C \cdots H/H \cdots C(core) and H \cdots H(edges) type. The intercentroid distance for rings that exhibit strong $\pi\cdots\pi$ interactions is 3.75 Å and these rings greatly overlap. Fig. 7*b* defines hollows toward the center of the molecule and bumps on the pyrene edges, confirming that intermolecular interactions allow molecules to interlock for the crystal packing,

Evaluation of the curvedness reflects the planarity of the pyrene rings, specifically for those exhibiting strong $\pi\cdots\pi$ interactions (Fig. 8*a*), while the other rings and solvent ligands have both flat and positive curvatures. Hence, compound **1** has diverse interactions that give way to the resulting array. Fig. 8*a* portrays a superposition of where the pyrene ring is located below the generated surface; only a green color (*i.e.*, flatness) is observed in this region. Going from Fig. 8*b* to Fig. 8*c*, the red boxes are localized to fit together interlocking pyrene moieties towards the innermost region of the molecule, highlighting complementarity in the crystal-packing array.

The fingerprint plot for compound **1** is symmetric, and contacts occur over a long range of distances (*i.e.*, d_e and d_i scale) for C \cdots H/H \cdots C (39.8%), H \cdots H (44.2%), and H \cdots O/O \cdots H (7.4%) type primarily. H \cdots H contacts make up almost half the total interactions (44.2%). A large concentration of points is centered around 1.6–2.0 Å, linked to $\pi\cdots\pi$ stacking; contacts of C \cdots C (7.3%) type comprise DMSO–pyrene and pyrene–pyrene. Furthermore, characteristic traits are distinguished: both peaks and wings are demarcated in the C \cdots H/H \cdots C, H \cdots H, and H \cdots O/O \cdots H plots, so different contacts are present; they all incorporate the pyrene moieties and

**Figure 8**

Hirshfeld surface evaluated over curvedness for title compound **1**, viewed from the side (*a*) and top (*b*, *c*).

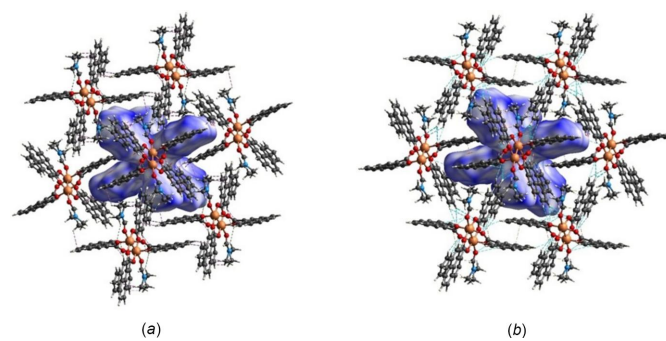
**Figure 9**

Fingerprint plot analysis for title compound **1**.

solvent ligands. Upon further analysis, it was found that DMSO participates in each type of contact in Fig. 9, either from the sulfur, oxygen, or methyl groups. Contacts of the C \cdots O/O \cdots C (0.1%), C \cdots S/S \cdots C (1.0%), and H \cdots S/S \cdots H (0.3%) types are not made out from short-contact interaction analysis because their distances are very long. Contacts of the C \cdots O/O \cdots C type arise from carboxylate and DMSO oxygen atoms to pyrene ring carbons, the C \cdots S/S \cdots C type go from the DMSO sulfur atom to pyrene ring carbons, and H \cdots S/S \cdots H from the DMSO sulfur atom to pyrene ring hydrogens.

The Hirshfeld surface generated for title compound **2** evaluated over d_{norm} shows the significance of the axial ligands as well as the pyrene moieties, like in compound **1**. As seen in Fig. 10, adjacent molecules surrounding the generated surface deliver multiple interactions, which are distributed from the innermost region near the oxygen atoms (*e.g.*, O₂ \cdots H34A at 2.79 Å, O₂ \cdots H34B at 2.61 Å), equatorial pyrene moieties (core and edges) (*e.g.*, C₄ \cdots C₄ at 3.18 Å, C₂₄ \cdots H16 at 2.70 Å), to the axial ligands (*e.g.*, H37B \cdots C16 at 2.87 Å).

Most of the red spots are intense (*i.e.*, short distance), mainly C \cdots C, H \cdots H, H \cdots O/O \cdots H, and C \cdots H/H \cdots C type interactions. However, just a few light-red spots (*i.e.*, longer distance) color are recognized as additional contacts, primarily C \cdots H/H \cdots C type. In Fig. 11, a few red spots are present on the pyrene aromatic core and most are located near the edges. In contrast, the DMF region has strong red spots. When comparing Fig. 6 and Fig. 11, the latter surface contains a

**Figure 10**

Hirshfeld surface evaluated over d_{norm} for title compound **2** with adjacent molecules showing short contacts (*a*) C \cdots H/H \cdots C (purple) and H \cdots H (green), (*b*) H \cdots O/O \cdots H (blue) and C \cdots C (orange).

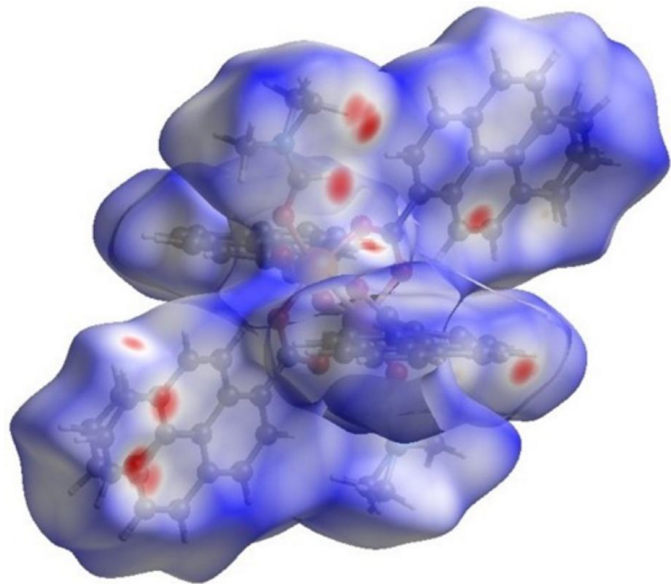


Figure 11
Hirshfeld surface evaluated over d_{norm} for title compound 2.

qualitatively greater amount of blue regions; however, the red spots are more intense, implying compound **1** has strong interactions distributed over more parts of the surface but compound **2** has shorter distances in most of its interactions.

Pyrene ring surfaces with red–yellow and blue–green adjacent triangles, as displayed in Fig. 12*a*, are characteristic of π – π interactions, which are expected due to the nature of the PAHs. Similar to compound **1**, not all rings show this degree of interaction because of the position of each pyrene ring with respect to other moieties in the crystal-packing array and corresponding interactions. Different from Fig. 7*a*, Fig. 12*a* has a less uniform pattern of π – π interactions than for title compound **1**, as a result of the less overlapping pyrene rings. Rings with weak π – π interactions have more C···H/H···C(core) and H···H(edges) contacts, analogous to compound **1**.

The planarity of the pyrene moieties is depicted by the curvedness (Fig. 13*a*) where most of the surface is flat. However, even pyrene rings that exhibit strong π – π interactions do not possess a completely flat surface region (unlike in compound **1**), and the other rings have alternating regions of flatness. The intercentroid distance for rings that exhibit strong π – π interactions is 5.83 Å, farther apart than for compound **1**. In addition, the red box in Fig. 13*b* can be

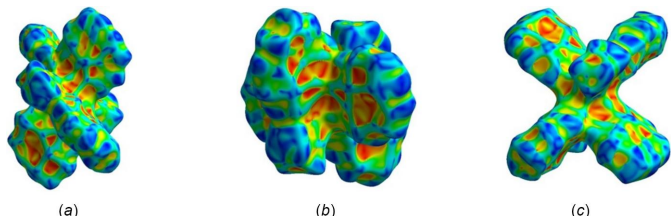


Figure 12
Hirshfeld surface evaluated over shape-index for title compound 2, viewed from the side (*a*), (*b*) and top (*c*).

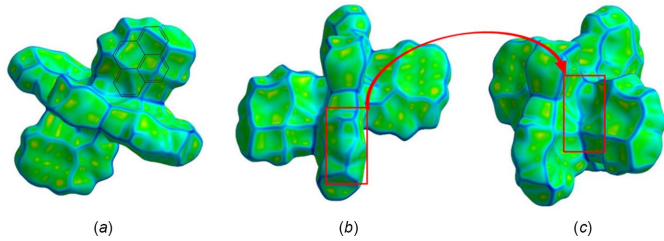


Figure 13
Hirshfeld surface evaluated over curvedness for title compound 2, viewed from the side (*a*) and top (*b*), (*c*).

translated into the one in Fig. 13*c*; thus, complementarity is observed within the generated surface, coming from intermolecular interactions that follow the screw axes and glide planes present in title compound **2** ($P2_1/n$). Both compounds achieve complementarity in their crystal packing, but each arises from different intermolecular interactions.

The 2D fingerprint plot for compound **2** (Fig. 14) has the following features: it is quasi-symmetric, C···H/H···C interactions account for almost half of the contacts (44.9%) followed by H···H (40.5%), with fewer contributions from H···O/O···H (10.7%) and C···C (3.4%) interactions. C···H/H···C contacts have broad peaks spread out over most of the plot, H···H contacts also cover a broad range of distances and several types of interactions, and H···O/O···H contacts have wide peaks and fewer weak contacts. In the same way as for compound **1**, all contacts in Fig. 14 include atoms from the solvent, DMF in the case of compound **2**. Likewise, contacts of the C···O/O···C (0.1%), C···N/N···C (0.4%), and H···N/N···H (0.1%) types are not identified from short-contact interaction analysis because the distances are long. Contacts of the C···O/O···C type arise from carboxylate and DMF oxygen atoms to pyrene ring carbons (as in compound **1**), the C···N/N···C type go from the DMF nitrogen atom to pyrene ring carbons, and H···N/N···H from the DMF nitrogen atom to pyrene ring hydrogens.

6. Database survey

A search of the Cambridge Structural Database (CSD Version 5.44, June 2023 update; Groom *et al.*, 2016) for the two

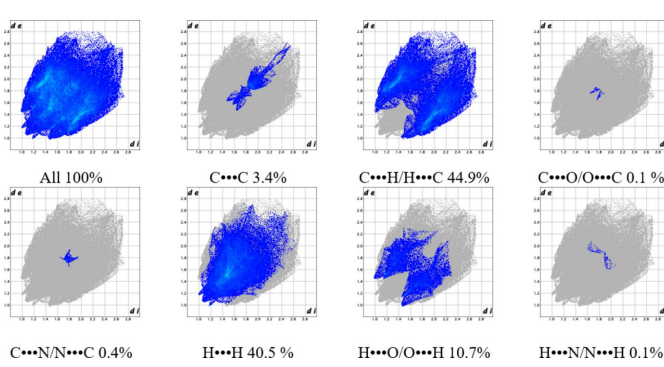


Figure 14
Fingerprint plot analysis for title compound 2.

Table 1

Experimental details.

	1	2
Crystal data		
Chemical formula	[Cu ₂ (C ₁₇ H ₉ O ₂) ₄ (C ₂ H ₆ OS) ₂]	[Cu ₂ (C ₁₇ H ₉ O ₂) ₄ (C ₃ H ₇ NO) ₂]
<i>M</i> _r	1264.30	1254.24
Crystal system, space group	Triclinic, <i>P</i> 1̄	Monoclinic, <i>P</i> 2 ₁ / <i>n</i>
Temperature (K)	100	300
<i>a</i> , <i>b</i> , <i>c</i> (Å)	10.5283 (1), 11.8583 (2), 11.9401 (1)	10.54266 (13), 21.8888 (2), 12.66517 (15)
α , β , γ (°)	101.044 (1), 98.136 (1), 104.142 (1)	90, 100.1160 (11), 90
<i>V</i> (Å ³)	1390.69 (3)	2877.25 (6)
<i>Z</i>	1	2
Radiation type	Cu <i>K</i> α	Cu <i>K</i> α
μ (mm ⁻¹)	2.19	1.46
Crystal size (mm)	0.12 × 0.11 × 0.09	0.12 × 0.08 × 0.04
Data collection		
Diffractometer	Rigaku SuperNova Hypix6000	Rigaku SuperNova Hypix6000
Absorption correction	Multi-scan (Blessing, 1995)	Multi-scan (Blessing, 1995)
<i>T</i> _{min} , <i>T</i> _{max}	0.778, 0.818	0.844, 0.944
No. of measured, independent and observed [<i>I</i> > 2σ(<i>I</i>)] reflections	78157, 5097, 4827	15433, 5246, 4485
<i>R</i> _{int}	0.048	0.023
(sin θ /λ) _{max} (Å ⁻¹)	0.604	0.603
Refinement		
<i>R</i> [<i>F</i> ² > 2σ(<i>F</i> ²)], <i>wR</i> (<i>F</i> ²), <i>S</i>	0.032, 0.082, 1.05	0.031, 0.091, 1.07
No. of reflections	5142	5246
No. of parameters	391	447
No. of restraints	0	1
H-atom treatment	H-atom parameters constrained	H-atom parameters constrained
Δρ _{max} , Δρ _{min} (e Å ⁻³)	0.45, -0.47	0.20, -0.28

Computer programs: *CrysAlis PRO* (Rigaku OD, 2020), *SHELXT* (Sheldrick, 2015a), *SHELXL2018/3* (Sheldrick, 2015b), and *OLEX2* (Dolomanov *et al.*, 2009).

reported compounds revealed a total of five hits containing polycyclic aromatic copper dimers. None of the these was an exact match to the pyrene moieties of the title compounds. Four of them included naphthalene moieties and the remaining structure contained phenanthrene. The four structures that contained naphthalene groups are *catena*-[tetrakis(μ₄-naphthalene-2,6-dicarboxylato)bis(μ₂-4,4'-bipyridine)tetra(copper(II) bis(μ₄-naphthalene-2,6-dicarboxylato)(μ₂-4,4'-bipyridine)dicopper(II)] (BUSQOW; Kanoo *et al.*, 2009), tetrakis(μ-naphthalene-2-carboxylato)bis(acetonitrile)dicopper acetonitrile solvate (CUJFAR; Liu *et al.*, 2020), tetrakis(μ-2-naphthoato)bis(acetonitrile)dicopper acetonitrile solvate (WUNRII; Goldberg *et al.*, 2015), and tetrakis(μ-2-naphthoato)bis(2,3-dimethylpyridine)dicopper (WUNROO; Goldberg *et al.*, 2015). The axial ligands present in CUJFAR, WUNRII, and WUNROO are involved in intermolecular interactions with adjacent molecules that contribute to the crystal-packing array. The naphthalene ligands in the above-mentioned structures participate in π–π interactions. Moreover, the nature of the axial ligands determines the contribution of π interactions to the crystal packing. For example, in WUNROO, the properties and position of the 2,3-lutidine (aromatic heterocycle molecule) allowed for enhanced π interactions. In contrast, CUJFAR and WUNRII contain acetonitrile (non-aromatic linear molecule) as their axial ligand and present mainly C···C and C···H interactions. Finally, the last hit, corresponding to tetrakis(μ₂-phenanthrene-9-carboxylato)bis(*N,N*-dimethylformamide)dicopper(II) (WUZCEA; Wang *et al.*, 2010) resembles title

compound **2** in having a phenanthrene instead of a pyrene equatorial ligand, resulting in a change of the space-group setting from *P*2₁/*c* (WUZCEA) to *P*2₁/*n* (**2**). In terms of the packing structure, WUZCEA exhibits fewer short contacts, C···C and O···H type interactions than compound **2**, which presents C···C, H···H, C···H, and O···H type interactions. Nonetheless, WUZCEA exhibits more π–π interactions than compound **2**. Similarly to the other compounds reported in this survey, in WUZCEA the axial ligands play an important role in the crystal packing of the molecules.

7. Synthesis and crystallization

All the chemicals were purchased from Sigma-Aldrich. The chemicals and solvents were used as supplied without further purification. IR spectra were recorded on a FT-IR Frontier Perkin Elmer spectrophotometer with ATR modality in the region 4000–600 cm⁻¹. UV-vis spectra were recorded on a UV-1900 spectrophotometer in the range 200–1000 nm using a 1 cm path-length cell for solution in DMSO or DMF. The CVs were recorded in a BioLogic potentiostat using a solution of 0.1 M TBAPF₆ with a glassy carbon working electrode, a graphite rod counter-electrode, and a 0.01 M AgNO₃ silver wire pseudo-reference electrode corrected with ferrocene.

Synthesis of [Cu₂(pyr-COO⁻)₄(DMSO)₂] (**1**):

1-Pyrene carboxylic acid (0.084 g, 0.3 mmol) was dissolved in 18 mL of methanol and deprotonated with triethylamine (0.034 g, 0.23 mmol). The pyrene-1-carboxylate solution was added slowly to a methanolic solution of Cu(NO₃)₂·H₂O

(0.0819 g, 0.033 mmol) at room temperature, which afforded a green solid. The mixture was stirred for 24 h and was then filtered out. The solid was dissolved in DMSO for crystallization. Single crystals were obtained by vapor diffusion of methanol into dimethyl sulfoxide after one week. Yield: (85.6 mg, 68%). IR (ATR); ν (cm⁻¹): 3041 (w), 1920 (w), 1672 (w), 1589 (s), 1506 (m), 1392 (s), 1359 (s), 1312 (m), 1165 (m), 838 (s), 710 (s), 619 (m). UV-vis; λ_{max} (DMSO, nm) 280 (pyr-COO) (Niko *et al.*, 2012; Johnpeter & Therrien, 2013), 335 (pyr-COO, π - π^* transition) (Haldar *et al.*, 2016), 352 (pyr-COO) (Niko *et al.*, 2012; Johnpeter & Therrien, 2013), 379 (pyr-COO) (Niko *et al.*, 2012; Johnpeter & Therrien, 2013), and 739 (Cu, *d-d* and MLCT transitions) (Wang *et al.*, 2021).

Synthesis of [Cu₂(pyr-COO⁻)₄(DMF)₂] (2):

A similar synthetic procedure as for **1** was used. However, the crystallization process was different. The resulting solid was dissolved in DMF for crystallization. Single crystals were obtained by vapor diffusion of methanol into dimethyl formamide after one week. Yield: (87.1 mg, 69%). IR (ATR); ν (cm⁻¹): 1655 (m), 1607(s), 1591 (s), 1385 (s), 1359 (s), 1314 (m), 1165 (m), 853 (s), 820 (s), 760 (s), 671 (m). UV-vis; λ_{max} (DMF, nm) 283 (pyr-COO) (Niko *et al.*, 2012; Johnpeter & Therrien, 2013), 337 (pyr-COO, π - π^* transitions) (Haldar *et al.*, 2016), 352 (pyr-COO) (Niko *et al.*, 2012; Johnpeter & Therrien, 2013), 382 (pyr-COO) (Niko *et al.*, 2012; Johnpeter & Therrien, 2013), and 701 (Cu, *d-d* and MLCT transitions) (Wang *et al.*, 2021).

8. Refinement

Crystal data, data collection and structure refinement details are summarized in Table 1. H atoms were included in geometrically calculated positions and refined as riding atoms with C—H = 0.93 Å and $U_{\text{iso}}(\text{H}) = 1.2U_{\text{eq}}(\text{C})$.

Acknowledgements

Author contributions: Conceptualization, DMPC and KGN; methodology, KGN, VCNG, VPMQ, PCRA and ACBJ; formal analysis, DMPC, ABS and JRR; investigation, DMPC and KGN; resources, DMPC and KGN; data curation, DMPC, ABS and JORR; writing-original draft preparation, DMPC, KGN, ABS, JORR and VCNG; writing-review and editing, DMPC and KGN; supervision, DMPC and KGN project administration, DMPC and KGN; funding acquisition, DMPC and KGN. All authors have read and agreed to published version of the manuscript. **Acknowledgments:** We would like to acknowledge the Department of Natural Sciences at UPR Carolina Campus (Department of Education, grant No. PO31S130068; however, these contents do not necessarily represent the policy of the Department of Education, and you should not assume endorsement by the Federal Government) and the University of Puerto Rico's Molecular Sciences Research Center for the use of the Rigaku XTLab SuperNova diffractometer (NSF CHE 1626103). Special thanks to Dr Logesh Mathivathanan for consultation on the final refinement of the structure.

Funding information

Funding for this research was provided by: National Science Foundation (award No. CHE-1626103); Puerto Rico Space Grant Consortium (award No. 80NSSC20M0053 to J.O.R.-R.).

References

- Aakeröy, C. A., Schultheiss, N. & Desper, J. (2006). *Dalton Trans.* pp. 1627–1635.
- Baldomá, R., Monfort, M., Ribas, J., Solans, X. & Maestro, M. A. (2006). *Inorg. Chem.* **45**, 8144–8155.
- Benesperi, I., Singh, R. & Marina, F. (2020). *Energies*, **13**, 2198.
- Blessing, R. H. (1995). *Acta Cryst. A* **51**, 33–38.
- Bonomo, R. P., Imperlizzeri, G., Pappalardo, G., Rizzarelli, E. & Tabbi, G. (2000). *Chemistry*, **6**, 4195–4202.
- Boulourani, Z., Katsamakas, S., Geromichalos, G. D., Psycharis, V., Raptopoulou, C. P., Hadjipavlou-Litina, D., Yiannaki, E. & Dendrinou-Samara, C. (2017). *Mater. Sci. Eng. C*, **76**, 1026–1040.
- Deacon, G. B. & Phillips, R. J. (1980). *Coord. Chem. Rev.* **33**, 227–250.
- Dolomanov, O. V., Bourhis, L. J., Gildea, R. J., Howard, J. A. K. & Puschmann, H. (2009). *J. Appl. Cryst.* **42**, 339–341.
- Elgrishi, N., Rountree, K. J., McCarthy, B. D., Rountree, E. S., Eisenhart, T. T. & Dempsey, J. L. (2018). *J. Chem. Educ.* **95**, 197–206.
- Goldberg, A. E., Kiskin, M. A., Nikolaevskii, S. A., Zorina-Tikhonova, E. N., Aleksandrov, G. G., Sidorov, A. A. & Eremenko, I. L. (2015). *Russ. J. Coord. Chem.* **41**, 163.
- Groom, C. R., Bruno, I. J., Lightfoot, M. P. & Ward, S. C. (2016). *Acta Cryst. B* **72**, 171–179.
- Guan, Q. L., Xing, Y. H., Liu, J., Han, C., Hou, C. Y. & Bai, F. Y. (2019). *J. Phys. Chem. C*, **123**, 23287–23296.
- Haldar, R., Heinke, L. & Wöll, C. (2020). *Adv. Mater.* **32**, 1905227–1905257.
- Haldar, R., Prasad, K., Samanta, P. K., Pati, S. & Maji, T. K. (2016). *Cryst. Growth Des.* **16**, 82–91.
- Iqbal, M., Ahmad, I., Ali, S., Muhammad, N., Ahmed, S. & Sohail, M. (2013). *Polyhedron*, **50**, 524–531.
- Johnpeter, J. P. & Therrien, B. (2013). *Inorg. Chim. Acta*, **405**, 437–443.
- Kanoo, P., Matsuda, M., Higuchi, M., Kitagawa, S. & Maji, T. K. (2009). *Chem. Mater.* **21**, 5860–5866.
- Karmakar, A., Paul, A., Sabatini, E. P., Guedes da Silva, M. F. C. & Pombeiro, A. J. L. (2021). *Molecules*, **26**, 1101.
- Kinik, F. P., Ortega-Guerrero, A., Ongari, D., Ireland, C. P. & Smit, B. (2021). *Chem. Soc. Rev.* **50**, 3143–3177.
- Kozlevčar, B., Leban, I., Petrič, M., Petriček, S., Roubeau, O., Reedijk, J. & Šegedin, P. (2004). *Inorg. Chim. Acta*, **357**, 4220–4230.
- Liu, K.-G., Yao, Z.-X., Li, J.-Z. & Yan, X.-W. (2020). *Inorg. Chim. Acta*, **508**, 119608.
- Modec, B., Podjed, N. & Lah, N. (2020). *Molecules*, **25**, 1573–1597.
- Murugavel, R., Karambelkar, V. V., Anantharaman, G. & Walawalkar, M. G. (2000). *Inorg. Chem.* **39**, 1381–1390.
- Niko, Y., Hiroshige, Y., Kawauchi, S. & Konishi, G. I. (2012). *Tetrahedron*, **68**, 6177–6185.
- Rajakannu, P., Kaleeswaran, D., Banerjee, S., Butcher, R. J. & Murugavel, R. (2019). *Inorg. Chim. Acta*, **486**, 283–293.
- Rao, C. N. R., Natarajan, S. & Vaidhyanathan, R. (2004). *Angew. Chem. Int. Ed.* **43**, 1466–1496.
- Rigaku OD (2020). *CrysAlis PRO*. Agilent Technologies Ltd, Yarnton, England.
- Seo, J. S., Whang, D., Lee, H., Jun, S. I., Oh, J., Jeon, Y. J. & Kim, K. (2000). *Nature*, **404**, 982–986.
- Sheldrick, G. M. (2015a). *Acta Cryst. A* **71**, 3–8.
- Sheldrick, G. M. (2015b). *Acta Cryst. C* **71**, 3–8.

- Spackman, M. A. & Jayatilaka, D. (2009). *CrystEngComm*, **11**, 19–32.
- Spackman, M. A. & McKinnon, J. J. (2002). *CrystEngComm*, **4**, 378–392.
- Spackman, P. R., Turner, M. J., McKinnon, J. J., Wolff, S. K., Grimwood, D. J., Jayatilaka, D. & Spackman, M. A. (2021). *J. Appl. Cryst.* **54**, 1006–1011.
- Turner, M. J., McKinnon, J. J., Wolff, S. K., Grimwood, D. J., Spackman, P. R., Jayatilaka, D. & Spackman, M. A. (2017). *CrystalExplorer17.5*. University of Western Australia.
- Vishnoi, P., Kaleeswaran, D. & Murugavel, R. (2017). *Chemistry Select*, **2**, 12014–12018.
- Wang, H. H., Li, J. Z., Nie, J., Yao, Z. X., Li, H. J., Liu, K. G. & Yan, X. W. (2021). *Inorg. Chim Acta*, **514**, 120018.
- Wang, J., Chang, Z., Zhang, A., Hu, T. & Bu, X. (2010). *Inorg. Chim. Acta*, **363**, 1377–1385.
- Wang, X., Zhao, W., Zhang, J. & Lu, Q. (2013). *J. Solid State Chem.* **198**, 162–168.
- Zhao, Y. L. & Stoddart, J. F. (2009). *Acc. Chem. Res.* **42**, 1161–1171.

supporting information

Acta Cryst. (2024). E80, 1-9 [https://doi.org/10.1107/S2056989023010277]

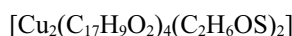
New copper carboxylate pyrene dimers: synthesis, crystal structure, Hirshfeld surface analysis and electrochemical characterization

Vianca C. Nogu  -Guzm  n, Alejandro Burgos-Suazo, Javier O. Rivera-Reyes, Vasti P. Montes Qui  ones, Paola C. Ramis-Aybar, Adriana C. Burgos-Jim  nez, Karilys Gonz  lez-Nieves and Dalice M. Pi  nero-Cruz

Computing details

Bis(dimethyl sulfoxide)tetrakis(  -pyrene-1-carboxylato)dicopper(Cu—Cu) (1)

Crystal data



$M_r = 1264.30$

Triclinic, $P\bar{1}$

$a = 10.5283 (1)$   

$b = 11.8583 (2)$   

$c = 11.9401 (1)$   

$\alpha = 101.044 (1)^\circ$

$\beta = 98.136 (1)^\circ$

$\gamma = 104.142 (1)^\circ$

$V = 1390.69 (3)$   ³

$Z = 1$

$F(000) = 650$

$D_x = 1.510 \text{ Mg m}^{-3}$

Cu $K\alpha$ radiation, $\lambda = 1.54184$   

Cell parameters from 5097 reflections

$\theta = 0.8\text{--}0.8^\circ$

$\mu = 2.19 \text{ mm}^{-1}$

$T = 100$ K

Block, green

$0.12 \times 0.11 \times 0.09$ mm

Data collection

Rigaku SuperNova Hypix6000
diffractometer

Radiation source: microsource

Detector resolution: 10.0000 pixels mm⁻¹

ω scans

Absorption correction: multi-scan
(Blessing, 1995)

$T_{\min} = 0.778$, $T_{\max} = 0.818$

78157 measured reflections

5097 independent reflections

4827 reflections with $I > 2\sigma(I)$

$R_{\text{int}} = 0.048$

$\theta_{\max} = 68.6^\circ$, $\theta_{\min} = 3.9^\circ$

$h = -12 \rightarrow 12$

$k = -11 \rightarrow 14$

$l = -14 \rightarrow 14$

Refinement

Refinement on F^2

Least-squares matrix: full

$R[F^2 > 2\sigma(F^2)] = 0.032$

$wR(F^2) = 0.082$

$S = 1.05$

5142 reflections

391 parameters

0 restraints

Hydrogen site location: inferred from
neighbouring sites

H-atom parameters constrained

$w = 1/[\sigma^2(F_o^2) + (0.0369P)^2 + 1.3914P]$
where $P = (F_o^2 + 2F_c^2)/3$

$(\Delta/\sigma)_{\max} = 0.001$

$\Delta\rho_{\max} = 0.45 \text{ e } \text{\AA}^{-3}$

$\Delta\rho_{\min} = -0.46 \text{ e } \text{\AA}^{-3}$

Extinction correction: *SHELXL2018/3*
(Sheldrick, 2015b),

$F_c^* = kFc[1 + 0.001xFc^2\lambda^3/\sin(2\theta)]^{1/4}$

Extinction coefficient: 0.00045 (11)

Special details

Geometry. All esds (except the esd in the dihedral angle between two l.s. planes) are estimated using the full covariance matrix. The cell esds are taken into account individually in the estimation of esds in distances, angles and torsion angles; correlations between esds in cell parameters are only used when they are defined by crystal symmetry. An approximate (isotropic) treatment of cell esds is used for estimating esds involving l.s. planes.

Fractional atomic coordinates and isotropic or equivalent isotropic displacement parameters (\AA^2)

	<i>x</i>	<i>y</i>	<i>z</i>	$U_{\text{iso}}^*/U_{\text{eq}}$
Cu1	0.91294 (2)	0.49438 (2)	0.40919 (2)	0.01418 (9)
S3	0.79851 (5)	0.59369 (4)	0.19711 (4)	0.02605 (13)
O1	0.82175 (13)	0.56000 (12)	0.52641 (11)	0.0228 (3)
O2	0.96841 (13)	0.56908 (13)	0.68455 (11)	0.0257 (3)
O3	0.82877 (13)	0.33234 (11)	0.42304 (11)	0.0229 (3)
O4	0.97457 (13)	0.34410 (12)	0.58282 (12)	0.0236 (3)
O5	0.76843 (12)	0.49904 (12)	0.26558 (11)	0.0223 (3)
C1	0.86206 (17)	0.58347 (16)	0.63416 (16)	0.0172 (4)
C2	0.77238 (18)	0.63064 (16)	0.70712 (16)	0.0179 (4)
C3	0.63637 (18)	0.59548 (17)	0.65730 (16)	0.0199 (4)
H3	0.606849	0.545289	0.580998	0.024*
C4	0.54310 (18)	0.63170 (16)	0.71598 (17)	0.0199 (4)
H4	0.450794	0.603095	0.681218	0.024*
C5	0.58426 (19)	0.70972 (17)	0.82549 (16)	0.0207 (4)
C6	0.72345 (19)	0.74971 (17)	0.87799 (16)	0.0193 (4)
C7	0.81763 (18)	0.70674 (17)	0.81909 (15)	0.0186 (4)
C8	0.95692 (19)	0.74954 (19)	0.87781 (17)	0.0256 (4)
H8	1.022196	0.723354	0.840727	0.031*
C9	0.9957 (2)	0.8256 (2)	0.98378 (17)	0.0294 (5)
H9	1.087549	0.850467	1.019974	0.035*
C10	0.9021 (2)	0.8703 (2)	1.04378 (17)	0.0281 (4)
C11	0.76560 (19)	0.83241 (18)	0.98852 (16)	0.0222 (4)
C12	0.6704 (2)	0.87714 (18)	1.04386 (17)	0.0237 (4)
C13	0.5324 (2)	0.83475 (19)	0.98846 (18)	0.0276 (4)
H13	0.468633	0.863931	1.025241	0.033*
C14	0.4911 (2)	0.75446 (18)	0.88537 (18)	0.0260 (4)
H14	0.398478	0.726802	0.851516	0.031*
C15	0.7158 (2)	0.9604 (2)	1.15152 (18)	0.0302 (5)
H15	0.653921	0.993068	1.187969	0.036*
C16	0.8488 (2)	0.9958 (2)	1.20560 (18)	0.0360 (5)
H16	0.877114	1.051076	1.279330	0.043*
C17	0.9414 (2)	0.9512 (2)	1.15288 (18)	0.0357 (5)
H17	1.032500	0.975761	1.191211	0.043*
C18	0.87448 (16)	0.28873 (16)	0.50314 (15)	0.0154 (4)
C19	0.81254 (17)	0.15973 (16)	0.50049 (15)	0.0153 (3)
C20	0.89333 (18)	0.10243 (17)	0.55814 (15)	0.0186 (4)
H20	0.976743	0.148747	0.606131	0.022*
C21	0.85498 (18)	-0.01959 (17)	0.54708 (16)	0.0194 (4)
H21	0.911828	-0.055685	0.587996	0.023*

C22	0.73365 (18)	-0.09086 (16)	0.47652 (15)	0.0180 (4)
C23	0.64539 (17)	-0.03391 (16)	0.42348 (15)	0.0154 (4)
C24	0.68319 (17)	0.09253 (16)	0.43646 (14)	0.0147 (3)
C25	0.58634 (17)	0.14480 (16)	0.38548 (15)	0.0169 (4)
H25	0.607986	0.229155	0.395251	0.020*
C26	0.46483 (17)	0.07596 (17)	0.32380 (15)	0.0180 (4)
H26	0.402257	0.113635	0.293537	0.022*
C27	0.42811 (17)	-0.05156 (17)	0.30298 (15)	0.0183 (4)
C28	0.51893 (17)	-0.10641 (16)	0.35411 (15)	0.0170 (4)
C29	0.48514 (19)	-0.23307 (17)	0.33528 (16)	0.0215 (4)
C30	0.3614 (2)	-0.30173 (18)	0.26544 (18)	0.0278 (4)
H30	0.337925	-0.386475	0.252135	0.033*
C31	0.2734 (2)	-0.24735 (19)	0.21585 (18)	0.0289 (5)
H31	0.190048	-0.295055	0.168667	0.035*
C32	0.30546 (19)	-0.12393 (18)	0.23425 (17)	0.0239 (4)
H32	0.243618	-0.087873	0.199899	0.029*
C33	0.5800 (2)	-0.28605 (17)	0.38834 (18)	0.0258 (4)
H33	0.559200	-0.370679	0.375341	0.031*
C34	0.6964 (2)	-0.21894 (17)	0.45530 (17)	0.0236 (4)
H34	0.756188	-0.256821	0.489781	0.028*
C35	0.8858 (3)	0.5371 (3)	0.0929 (2)	0.0514 (7)
H35A	0.970862	0.530951	0.132917	0.077*
H35B	0.902953	0.591272	0.040810	0.077*
H35C	0.831661	0.457693	0.047304	0.077*
C36	0.6437 (2)	0.5714 (2)	0.10162 (19)	0.0337 (5)
H36A	0.605648	0.486001	0.064883	0.051*
H36B	0.658719	0.616149	0.041424	0.051*
H36C	0.581536	0.599821	0.146035	0.051*

Atomic displacement parameters (\AA^2)

	U^{11}	U^{22}	U^{33}	U^{12}	U^{13}	U^{23}
Cu1	0.01343 (14)	0.01139 (15)	0.01692 (14)	0.00270 (10)	0.00178 (10)	0.00332 (10)
S3	0.0222 (2)	0.0246 (3)	0.0284 (3)	0.00069 (19)	-0.00273 (18)	0.0127 (2)
O1	0.0253 (7)	0.0281 (8)	0.0213 (7)	0.0164 (6)	0.0077 (5)	0.0066 (6)
O2	0.0232 (7)	0.0341 (8)	0.0196 (6)	0.0117 (6)	0.0046 (5)	0.0008 (6)
O3	0.0241 (7)	0.0138 (7)	0.0260 (7)	-0.0003 (5)	-0.0032 (5)	0.0067 (5)
O4	0.0217 (6)	0.0179 (7)	0.0260 (7)	-0.0020 (5)	-0.0037 (5)	0.0087 (5)
O5	0.0172 (6)	0.0246 (7)	0.0240 (7)	0.0019 (5)	-0.0011 (5)	0.0117 (6)
C1	0.0183 (9)	0.0105 (8)	0.0233 (9)	0.0034 (7)	0.0065 (7)	0.0043 (7)
C2	0.0205 (9)	0.0149 (9)	0.0216 (9)	0.0071 (7)	0.0065 (7)	0.0077 (7)
C3	0.0200 (9)	0.0160 (9)	0.0247 (9)	0.0043 (7)	0.0050 (7)	0.0076 (8)
C4	0.0161 (8)	0.0166 (9)	0.0286 (10)	0.0045 (7)	0.0046 (7)	0.0093 (8)
C5	0.0230 (9)	0.0170 (9)	0.0261 (9)	0.0065 (8)	0.0085 (7)	0.0105 (8)
C6	0.0246 (9)	0.0177 (9)	0.0207 (9)	0.0088 (8)	0.0093 (7)	0.0095 (7)
C7	0.0230 (9)	0.0174 (9)	0.0194 (9)	0.0085 (7)	0.0075 (7)	0.0079 (7)
C8	0.0227 (10)	0.0317 (11)	0.0230 (9)	0.0110 (8)	0.0051 (8)	0.0031 (8)
C9	0.0214 (9)	0.0411 (13)	0.0223 (10)	0.0119 (9)	-0.0006 (8)	-0.0010 (9)

C10	0.0281 (10)	0.0356 (12)	0.0237 (10)	0.0144 (9)	0.0051 (8)	0.0070 (9)
C11	0.0269 (10)	0.0230 (10)	0.0212 (9)	0.0104 (8)	0.0089 (8)	0.0082 (8)
C12	0.0307 (10)	0.0239 (10)	0.0226 (9)	0.0119 (8)	0.0120 (8)	0.0096 (8)
C13	0.0272 (10)	0.0292 (11)	0.0344 (11)	0.0127 (9)	0.0158 (9)	0.0130 (9)
C14	0.0228 (9)	0.0246 (11)	0.0347 (11)	0.0073 (8)	0.0104 (8)	0.0126 (9)
C15	0.0354 (11)	0.0349 (12)	0.0251 (10)	0.0148 (10)	0.0135 (9)	0.0065 (9)
C16	0.0412 (12)	0.0446 (14)	0.0207 (10)	0.0166 (11)	0.0057 (9)	-0.0016 (9)
C17	0.0319 (11)	0.0498 (15)	0.0235 (10)	0.0167 (10)	0.0020 (9)	-0.0007 (10)
C18	0.0149 (8)	0.0150 (9)	0.0174 (8)	0.0058 (7)	0.0062 (7)	0.0022 (7)
C19	0.0171 (8)	0.0128 (9)	0.0160 (8)	0.0044 (7)	0.0052 (7)	0.0019 (7)
C20	0.0168 (8)	0.0188 (9)	0.0199 (9)	0.0053 (7)	0.0027 (7)	0.0035 (7)
C21	0.0199 (9)	0.0199 (10)	0.0225 (9)	0.0099 (7)	0.0051 (7)	0.0080 (8)
C22	0.0219 (9)	0.0158 (9)	0.0199 (9)	0.0079 (7)	0.0086 (7)	0.0061 (7)
C23	0.0173 (8)	0.0143 (9)	0.0157 (8)	0.0049 (7)	0.0066 (7)	0.0033 (7)
C24	0.0167 (8)	0.0136 (9)	0.0150 (8)	0.0050 (7)	0.0065 (6)	0.0028 (7)
C25	0.0192 (8)	0.0133 (9)	0.0201 (9)	0.0058 (7)	0.0063 (7)	0.0052 (7)
C26	0.0175 (8)	0.0201 (10)	0.0206 (9)	0.0087 (7)	0.0061 (7)	0.0082 (7)
C27	0.0172 (8)	0.0198 (10)	0.0176 (8)	0.0036 (7)	0.0055 (7)	0.0041 (7)
C28	0.0184 (8)	0.0151 (9)	0.0179 (8)	0.0039 (7)	0.0071 (7)	0.0036 (7)
C29	0.0239 (9)	0.0166 (10)	0.0232 (9)	0.0032 (8)	0.0071 (7)	0.0038 (8)
C30	0.0294 (10)	0.0152 (10)	0.0331 (11)	-0.0008 (8)	0.0053 (8)	0.0016 (8)
C31	0.0210 (9)	0.0255 (11)	0.0314 (11)	-0.0020 (8)	0.0000 (8)	0.0005 (9)
C32	0.0202 (9)	0.0255 (11)	0.0239 (9)	0.0048 (8)	0.0021 (7)	0.0045 (8)
C33	0.0350 (11)	0.0126 (9)	0.0333 (11)	0.0083 (8)	0.0128 (9)	0.0074 (8)
C34	0.0310 (10)	0.0167 (10)	0.0295 (10)	0.0126 (8)	0.0105 (8)	0.0098 (8)
C35	0.0459 (14)	0.077 (2)	0.0506 (15)	0.0258 (14)	0.0248 (12)	0.0384 (15)
C36	0.0270 (11)	0.0388 (13)	0.0342 (11)	0.0053 (9)	-0.0054 (9)	0.0195 (10)

Geometric parameters (\AA , ^\circ)

Cu1—Cu1 ⁱ	2.5934 (5)	C16—H16	0.9500
Cu1—O1	1.9530 (13)	C16—C17	1.387 (3)
Cu1—O2 ⁱ	1.9779 (13)	C17—H17	0.9500
Cu1—O3	1.9586 (13)	C18—C19	1.502 (2)
Cu1—O4 ⁱ	1.9672 (13)	C19—C20	1.398 (3)
Cu1—O5	2.1441 (12)	C19—C24	1.420 (2)
S3—O5	1.5098 (13)	C20—H20	0.9500
S3—C35	1.774 (3)	C20—C21	1.379 (3)
S3—C36	1.782 (2)	C21—H21	0.9500
O1—C1	1.250 (2)	C21—C22	1.397 (3)
O2—C1	1.260 (2)	C22—C23	1.423 (2)
O3—C18	1.263 (2)	C22—C34	1.435 (3)
O4—C18	1.259 (2)	C23—C24	1.426 (3)
C1—C2	1.506 (2)	C23—C28	1.433 (2)
C2—C3	1.397 (3)	C24—C25	1.439 (2)
C2—C7	1.406 (3)	C25—H25	0.9500
C3—H3	0.9500	C25—C26	1.356 (3)
C3—C4	1.388 (3)	C26—H26	0.9500

C4—H4	0.9500	C26—C27	1.429 (3)
C4—C5	1.391 (3)	C27—C28	1.414 (3)
C5—C6	1.432 (3)	C27—C32	1.402 (3)
C5—C14	1.436 (3)	C28—C29	1.421 (3)
C6—C7	1.430 (3)	C29—C30	1.403 (3)
C6—C11	1.423 (3)	C29—C33	1.440 (3)
C7—C8	1.452 (3)	C30—H30	0.9500
C8—H8	0.9500	C30—C31	1.381 (3)
C8—C9	1.348 (3)	C31—H31	0.9500
C9—H9	0.9500	C31—C32	1.385 (3)
C9—C10	1.440 (3)	C32—H32	0.9500
C10—C11	1.416 (3)	C33—H33	0.9500
C10—C17	1.401 (3)	C33—C34	1.333 (3)
C11—C12	1.427 (3)	C34—H34	0.9500
C12—C13	1.429 (3)	C35—H35A	0.9800
C12—C15	1.402 (3)	C35—H35B	0.9800
C13—H13	0.9500	C35—H35C	0.9800
C13—C14	1.345 (3)	C36—H36A	0.9800
C14—H14	0.9500	C36—H36B	0.9800
C15—H15	0.9500	C36—H36C	0.9800
C15—C16	1.381 (3)		
O1—Cu1—Cu1 ⁱ	82.80 (4)	C15—C16—C17	120.4 (2)
O1—Cu1—O2 ⁱ	169.36 (5)	C17—C16—H16	119.8
O1—Cu1—O3	90.10 (6)	C10—C17—H17	119.6
O1—Cu1—O4 ⁱ	90.57 (6)	C16—C17—C10	120.8 (2)
O1—Cu1—O5	93.90 (5)	C16—C17—H17	119.6
O2 ⁱ —Cu1—Cu1 ⁱ	86.57 (4)	O3—C18—C19	118.75 (15)
O2 ⁱ —Cu1—O5	96.67 (5)	O4—C18—O3	124.48 (16)
O3—Cu1—Cu1 ⁱ	85.59 (4)	O4—C18—C19	116.65 (15)
O3—Cu1—O2 ⁱ	89.71 (6)	C20—C19—C18	116.52 (15)
O3—Cu1—O4 ⁱ	169.21 (5)	C20—C19—C24	119.37 (16)
O3—Cu1—O5	97.61 (5)	C24—C19—C18	123.93 (16)
O4 ⁱ —Cu1—Cu1 ⁱ	83.81 (4)	C19—C20—H20	119.2
O4 ⁱ —Cu1—O2 ⁱ	87.65 (6)	C21—C20—C19	121.65 (17)
O4 ⁱ —Cu1—O5	93.09 (5)	C21—C20—H20	119.2
O5—Cu1—Cu1 ⁱ	175.43 (4)	C20—C21—H21	119.6
O5—S3—C35	104.69 (11)	C20—C21—C22	120.87 (17)
O5—S3—C36	104.05 (9)	C22—C21—H21	119.6
C35—S3—C36	98.32 (12)	C21—C22—C23	118.55 (17)
C1—O1—Cu1	125.53 (12)	C21—C22—C34	122.07 (17)
C1—O2—Cu1 ⁱ	119.65 (12)	C23—C22—C34	119.38 (17)
C18—O3—Cu1	122.16 (11)	C22—C23—C24	120.75 (16)
C18—O4—Cu1 ⁱ	123.81 (12)	C22—C23—C28	118.73 (16)
S3—O5—Cu1	121.12 (7)	C24—C23—C28	120.49 (16)
O1—C1—O2	125.44 (16)	C19—C24—C23	118.40 (16)
O1—C1—C2	115.73 (15)	C19—C24—C25	123.84 (16)
O2—C1—C2	118.82 (16)	C23—C24—C25	117.75 (16)

C3—C2—C1	116.26 (16)	C24—C25—H25	119.4
C3—C2—C7	119.57 (17)	C26—C25—C24	121.27 (17)
C7—C2—C1	124.17 (16)	C26—C25—H25	119.4
C2—C3—H3	119.0	C25—C26—H26	119.0
C4—C3—C2	121.93 (18)	C25—C26—C27	121.94 (17)
C4—C3—H3	119.0	C27—C26—H26	119.0
C3—C4—H4	119.9	C28—C27—C26	118.59 (16)
C3—C4—C5	120.23 (17)	C32—C27—C26	122.41 (17)
C5—C4—H4	119.9	C32—C27—C28	119.00 (18)
C4—C5—C6	119.22 (17)	C27—C28—C23	119.75 (17)
C4—C5—C14	121.52 (17)	C27—C28—C29	119.92 (17)
C6—C5—C14	119.22 (18)	C29—C28—C23	120.33 (17)
C7—C6—C5	119.90 (17)	C28—C29—C33	118.50 (17)
C11—C6—C5	119.03 (17)	C30—C29—C28	118.98 (18)
C11—C6—C7	121.07 (17)	C30—C29—C33	122.51 (18)
C2—C7—C6	119.02 (17)	C29—C30—H30	119.7
C2—C7—C8	123.80 (17)	C31—C30—C29	120.68 (19)
C6—C7—C8	117.12 (17)	C31—C30—H30	119.7
C7—C8—H8	119.3	C30—C31—H31	119.7
C9—C8—C7	121.48 (18)	C30—C31—C32	120.63 (18)
C9—C8—H8	119.3	C32—C31—H31	119.7
C8—C9—H9	119.0	C27—C32—H32	119.6
C8—C9—C10	122.02 (19)	C31—C32—C27	120.79 (19)
C10—C9—H9	119.0	C31—C32—H32	119.6
C11—C10—C9	118.25 (18)	C29—C33—H33	119.3
C17—C10—C9	122.62 (19)	C34—C33—C29	121.45 (18)
C17—C10—C11	119.11 (19)	C34—C33—H33	119.3
C6—C11—C12	120.06 (18)	C22—C34—H34	119.2
C10—C11—C6	120.03 (17)	C33—C34—C22	121.56 (18)
C10—C11—C12	119.91 (18)	C33—C34—H34	119.2
C11—C12—C13	119.04 (18)	S3—C35—H35A	109.5
C15—C12—C11	118.54 (19)	S3—C35—H35B	109.5
C15—C12—C13	122.42 (18)	S3—C35—H35C	109.5
C12—C13—H13	119.3	H35A—C35—H35B	109.5
C14—C13—C12	121.39 (18)	H35A—C35—H35C	109.5
C14—C13—H13	119.3	H35B—C35—H35C	109.5
C5—C14—H14	119.4	S3—C36—H36A	109.5
C13—C14—C5	121.22 (19)	S3—C36—H36B	109.5
C13—C14—H14	119.4	S3—C36—H36C	109.5
C12—C15—H15	119.4	H36A—C36—H36B	109.5
C16—C15—C12	121.21 (19)	H36A—C36—H36C	109.5
C16—C15—H15	119.4	H36B—C36—H36C	109.5
C15—C16—H16	119.8		
Cu1—O1—C1—O2	0.3 (3)	C13—C12—C15—C16	177.1 (2)
Cu1—O1—C1—C2	-178.52 (11)	C14—C5—C6—C7	-179.52 (16)
Cu1 ⁱ —O2—C1—O1	0.5 (3)	C14—C5—C6—C11	0.3 (3)
Cu1 ⁱ —O2—C1—C2	179.35 (12)	C15—C12—C13—C14	-179.7 (2)

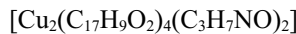
Cu1—O3—C18—O4	1.9 (2)	C15—C16—C17—C10	0.5 (4)
Cu1—O3—C18—C19	-173.80 (11)	C17—C10—C11—C6	-179.6 (2)
Cu1 ⁱ —O4—C18—O3	-4.8 (3)	C17—C10—C11—C12	0.3 (3)
Cu1 ⁱ —O4—C18—C19	171.03 (11)	C18—C19—C20—C21	-170.08 (16)
O1—C1—C2—C3	27.4 (2)	C18—C19—C24—C23	168.60 (15)
O1—C1—C2—C7	-152.14 (18)	C18—C19—C24—C25	-12.7 (3)
O2—C1—C2—C3	-151.58 (17)	C19—C20—C21—C22	0.6 (3)
O2—C1—C2—C7	28.9 (3)	C19—C24—C25—C26	179.09 (16)
O3—C18—C19—C20	155.26 (16)	C20—C19—C24—C23	-6.3 (2)
O3—C18—C19—C24	-19.7 (2)	C20—C19—C24—C25	172.45 (16)
O4—C18—C19—C20	-20.8 (2)	C20—C21—C22—C23	-4.9 (3)
O4—C18—C19—C24	164.21 (16)	C20—C21—C22—C34	174.44 (17)
C1—C2—C3—C4	179.28 (16)	C21—C22—C23—C24	3.6 (2)
C1—C2—C7—C6	177.40 (16)	C21—C22—C23—C28	-177.99 (16)
C1—C2—C7—C8	0.3 (3)	C21—C22—C34—C33	179.60 (18)
C2—C3—C4—C5	3.1 (3)	C22—C23—C24—C19	1.9 (2)
C2—C7—C8—C9	177.8 (2)	C22—C23—C24—C25	-176.86 (15)
C3—C2—C7—C6	-2.1 (3)	C22—C23—C28—C27	178.38 (15)
C3—C2—C7—C8	-179.20 (18)	C22—C23—C28—C29	-2.4 (2)
C3—C4—C5—C6	-1.5 (3)	C23—C22—C34—C33	-1.0 (3)
C3—C4—C5—C14	176.21 (17)	C23—C24—C25—C26	-2.2 (2)
C4—C5—C6—C7	-1.7 (3)	C23—C28—C29—C30	-179.02 (17)
C4—C5—C6—C11	178.10 (17)	C23—C28—C29—C33	0.6 (3)
C4—C5—C14—C13	-176.44 (19)	C24—C19—C20—C21	5.2 (3)
C5—C6—C7—C2	3.5 (3)	C24—C23—C28—C27	-3.2 (2)
C5—C6—C7—C8	-179.18 (17)	C24—C23—C28—C29	175.97 (16)
C5—C6—C11—C10	178.02 (18)	C24—C25—C26—C27	-2.0 (3)
C5—C6—C11—C12	-1.9 (3)	C25—C26—C27—C28	3.7 (3)
C6—C5—C14—C13	1.3 (3)	C25—C26—C27—C32	-176.59 (17)
C6—C7—C8—C9	0.6 (3)	C26—C27—C28—C23	-1.0 (2)
C6—C11—C12—C13	2.0 (3)	C26—C27—C28—C29	179.83 (16)
C6—C11—C12—C15	-178.66 (18)	C26—C27—C32—C31	179.91 (18)
C7—C2—C3—C4	-1.2 (3)	C27—C28—C29—C30	0.2 (3)
C7—C6—C11—C10	-2.2 (3)	C27—C28—C29—C33	179.83 (16)
C7—C6—C11—C12	177.90 (17)	C28—C23—C24—C19	-176.43 (15)
C7—C8—C9—C10	-1.1 (3)	C28—C23—C24—C25	4.8 (2)
C8—C9—C10—C11	0.0 (3)	C28—C27—C32—C31	-0.3 (3)
C8—C9—C10—C17	-178.7 (2)	C28—C29—C30—C31	-0.2 (3)
C9—C10—C11—C6	1.7 (3)	C28—C29—C33—C34	1.0 (3)
C9—C10—C11—C12	-178.40 (19)	C29—C30—C31—C32	-0.1 (3)
C9—C10—C17—C16	177.4 (2)	C29—C33—C34—C22	-0.8 (3)
C10—C11—C12—C13	-177.94 (19)	C30—C29—C33—C34	-179.34 (19)
C10—C11—C12—C15	1.4 (3)	C30—C31—C32—C27	0.4 (3)
C11—C6—C7—C2	-176.30 (17)	C32—C27—C28—C23	179.27 (16)
C11—C6—C7—C8	1.0 (3)	C32—C27—C28—C29	0.1 (3)
C11—C10—C17—C16	-1.3 (4)	C33—C29—C30—C31	-179.79 (19)
C11—C12—C13—C14	-0.4 (3)	C34—C22—C23—C24	-175.77 (16)
C11—C12—C15—C16	-2.3 (3)	C34—C22—C23—C28	2.6 (2)

C12—C13—C14—C5	−1.3 (3)	C35—S3—O5—Cu1	84.29 (13)
C12—C15—C16—C17	1.3 (4)	C36—S3—O5—Cu1	−173.01 (10)

Symmetry code: (i) $-x+2, -y+1, -z+1$.

Bis(dimethylformamide)tetrakis(μ -pyrene-1-carboxylato)dicopper(Cu—Cu) (2)

Crystal data



$M_r = 1254.24$

Monoclinic, $P2_1/n$

$a = 10.54266$ (13) Å

$b = 21.8888$ (2) Å

$c = 12.66517$ (15) Å

$\beta = 100.1160$ (11)°

$V = 2877.25$ (6) Å³

$Z = 2$

$F(000) = 1292$

$D_x = 1.448 \text{ Mg m}^{-3}$

Cu $K\alpha$ radiation, $\lambda = 1.54184$ Å

Cell parameters from 4485 reflections

$\theta = 0.9\text{--}0.9^\circ$

$\mu = 1.46 \text{ mm}^{-1}$

$T = 300$ K

Block, green

0.12 × 0.08 × 0.04 mm

Data collection

Rigaku SuperNova Hypix6000

diffractometer

Radiation source: microsource

Detector resolution: 10.0000 pixels mm^{−1}

ω scans

Absorption correction: multi-scan

(Blessing, 1995)

$T_{\min} = 0.844$, $T_{\max} = 0.944$

15433 measured reflections

5246 independent reflections

4485 reflections with $I > 2\sigma(I)$

$R_{\text{int}} = 0.023$

$\theta_{\max} = 68.4^\circ$, $\theta_{\min} = 4.0^\circ$

$h = -12 \rightarrow 10$

$k = -26 \rightarrow 26$

$l = -13 \rightarrow 15$

Refinement

Refinement on F^2

Least-squares matrix: full

$R[F^2 > 2\sigma(F^2)] = 0.031$

$wR(F^2) = 0.091$

$S = 1.07$

5246 reflections

447 parameters

1 restraint

Hydrogen site location: inferred from neighbouring sites

H-atom parameters constrained

$w = 1/[\sigma^2(F_o^2) + (0.0491P)^2 + 0.4863P]$

where $P = (F_o^2 + 2F_c^2)/3$

$(\Delta/\sigma)_{\max} = 0.001$

$\Delta\rho_{\max} = 0.20 \text{ e \AA}^{-3}$

$\Delta\rho_{\min} = -0.28 \text{ e \AA}^{-3}$

Special details

Geometry. All esds (except the esd in the dihedral angle between two l.s. planes) are estimated using the full covariance matrix. The cell esds are taken into account individually in the estimation of esds in distances, angles and torsion angles; correlations between esds in cell parameters are only used when they are defined by crystal symmetry. An approximate (isotropic) treatment of cell esds is used for estimating esds involving l.s. planes.

Fractional atomic coordinates and isotropic or equivalent isotropic displacement parameters (Å²)

	<i>x</i>	<i>y</i>	<i>z</i>	$U_{\text{iso}}^*/U_{\text{eq}}$	Occ. (<1)
Cu1	0.10029 (2)	0.46339 (2)	0.01883 (2)	0.03473 (9)	
O1	−0.04514 (13)	0.55286 (6)	−0.15584 (11)	0.0493 (3)	
O2	0.12690 (14)	0.49169 (7)	−0.12241 (11)	0.0535 (4)	
O3	0.03477 (13)	0.59478 (6)	0.04766 (13)	0.0547 (4)	
O4	0.20382 (12)	0.53317 (6)	0.08069 (12)	0.0503 (3)	
O5	0.24588 (12)	0.39180 (6)	0.04172 (11)	0.0495 (3)	

N1	0.2843 (2)	0.29133 (9)	0.0207 (2)	0.0861 (7)
C1	0.05677 (18)	0.53058 (8)	-0.17817 (15)	0.0413 (4)
C2	0.09464 (19)	0.55034 (9)	-0.28124 (15)	0.0434 (4)
C3	-0.0038 (2)	0.55820 (11)	-0.36868 (17)	0.0550 (5)
H3	-0.089016	0.555364	-0.358896	0.066*
C4	0.0220 (2)	0.57005 (12)	-0.46922 (17)	0.0609 (6)
H4	-0.045814	0.575850	-0.526110	0.073*
C5	0.1484 (2)	0.57351 (10)	-0.48705 (16)	0.0516 (5)
C6	0.25011 (19)	0.56952 (8)	-0.39786 (15)	0.0425 (4)
C7	0.22369 (18)	0.55878 (8)	-0.29303 (14)	0.0406 (4)
C8	0.3304 (2)	0.55944 (10)	-0.20505 (16)	0.0492 (5)
H8	0.314692	0.554463	-0.135557	0.059*
C9	0.4526 (2)	0.56709 (10)	-0.22076 (18)	0.0559 (5)
H9	0.519035	0.567719	-0.161763	0.067*
C10	0.4827 (2)	0.57427 (10)	-0.32593 (18)	0.0541 (5)
C11	0.3803 (2)	0.57542 (9)	-0.41406 (16)	0.0477 (5)
C12	0.4058 (2)	0.58161 (11)	-0.51984 (18)	0.0590 (6)
C13	0.5344 (3)	0.58709 (14)	-0.5332 (2)	0.0805 (8)
H13	0.553111	0.591080	-0.601975	0.097*
C14	0.6329 (3)	0.58669 (16)	-0.4474 (3)	0.0885 (9)
H14	0.717268	0.590893	-0.458614	0.106*
C15	0.6092 (2)	0.58014 (13)	-0.3441 (2)	0.0735 (7)
H15	0.677486	0.579644	-0.286562	0.088*
C16	0.3008 (3)	0.58189 (13)	-0.60718 (19)	0.0714 (7)
H16	0.317731	0.583965	-0.676722	0.086*
C17	0.1801 (3)	0.57930 (12)	-0.59274 (17)	0.0649 (6)
H17	0.114073	0.581250	-0.651932	0.078*
C18	0.15237 (17)	0.58494 (8)	0.07943 (14)	0.0390 (4)
C19	0.23279 (18)	0.63965 (8)	0.11993 (14)	0.0409 (4)
C20	0.1663 (2)	0.69272 (10)	0.1372 (2)	0.0586 (5)
H20	0.077020	0.693114	0.118151	0.070*
C21	0.2276 (2)	0.74439 (10)	0.1813 (2)	0.0676 (6)
H21	0.179776	0.779236	0.189580	0.081*
C22	0.3608 (2)	0.74503 (10)	0.21386 (19)	0.0568 (5)
C23	0.43190 (18)	0.69221 (8)	0.19576 (16)	0.0446 (4)
C24	0.36931 (17)	0.63922 (8)	0.14546 (14)	0.0386 (4)
C25	0.44932 (18)	0.58915 (9)	0.12436 (16)	0.0463 (4)
H25	0.411076	0.554935	0.088547	0.056*
C26	0.5787 (2)	0.59043 (10)	0.15518 (18)	0.0529 (5)
H26	0.627295	0.557535	0.138365	0.064*
C27	0.6423 (2)	0.64062 (10)	0.2125 (2)	0.0576 (5)
C28	0.5683 (2)	0.69203 (9)	0.23145 (19)	0.0545 (5)
C30	0.5536 (3)	0.79524 (12)	0.3041 (3)	0.0912 (10)
H30	0.592741	0.828210	0.343260	0.109*
H30A	0.593911	0.829460	0.338355	0.109*
C31	0.4277 (3)	0.79689 (11)	0.2668 (3)	0.0789 (8)
H31	0.381905	0.832360	0.275001	0.095*
C35	0.2118 (2)	0.34049 (11)	0.0132 (2)	0.0745 (7)

H35	0.125485	0.335492	-0.017035	0.089*	
C36	0.4184 (3)	0.29451 (15)	0.0634 (3)	0.0917 (9)	
H36A	0.433205	0.280956	0.136652	0.138*	
H36B	0.447514	0.335928	0.060275	0.138*	
H36C	0.465031	0.268801	0.022143	0.138*	
C29A	0.6250 (15)	0.7471 (9)	0.2866 (17)	0.081 (4)	0.65 (3)
C32A	0.7569 (13)	0.7376 (6)	0.3409 (17)	0.094 (4)	0.65 (3)
H32A	0.795517	0.767020	0.388907	0.112*	0.65 (3)
C33A	0.8273 (12)	0.6859 (6)	0.3235 (18)	0.107 (4)	0.65 (3)
H33A	0.914060	0.683192	0.354053	0.128*	0.65 (3)
C34A	0.7689 (13)	0.6389 (5)	0.2613 (15)	0.077 (4)	0.65 (3)
H34A	0.817416	0.604509	0.251930	0.092*	0.65 (3)
C37A	0.225 (3)	0.2297 (6)	0.014 (3)	0.119 (6)	0.45 (5)
H37A	0.133542	0.233293	-0.005127	0.179*	0.45 (5)
H37B	0.246498	0.209958	0.082987	0.179*	0.45 (5)
H37C	0.258081	0.205900	-0.038534	0.179*	0.45 (5)
C29B	0.636 (3)	0.7361 (17)	0.292 (3)	0.072 (5)	0.35 (3)
C32B	0.771 (2)	0.7459 (12)	0.294 (2)	0.083 (5)	0.35 (3)
H32B	0.808613	0.784346	0.306880	0.099*	0.35 (3)
C33B	0.8402 (19)	0.6974 (11)	0.278 (2)	0.083 (5)	0.35 (3)
H33B	0.929280	0.699307	0.298159	0.099*	0.35 (3)
C34B	0.786 (2)	0.6436 (12)	0.233 (2)	0.071 (5)	0.35 (3)
H34B	0.835839	0.611319	0.215515	0.085*	0.35 (3)
C37B	0.2384 (17)	0.2354 (9)	-0.043 (3)	0.138 (7)	0.55 (5)
H37D	0.208109	0.205937	0.003176	0.208*	0.55 (5)
H37E	0.308233	0.218162	-0.072421	0.208*	0.55 (5)
H37F	0.169484	0.246163	-0.099867	0.208*	0.55 (5)

Atomic displacement parameters (\AA^2)

	U^{11}	U^{22}	U^{33}	U^{12}	U^{13}	U^{23}
Cu1	0.03029 (14)	0.02935 (14)	0.04509 (16)	0.00122 (10)	0.00818 (10)	0.00401 (10)
O1	0.0472 (8)	0.0509 (8)	0.0537 (8)	0.0076 (6)	0.0190 (6)	0.0130 (6)
O2	0.0561 (8)	0.0551 (8)	0.0540 (8)	0.0164 (7)	0.0231 (7)	0.0145 (7)
O3	0.0357 (7)	0.0412 (7)	0.0818 (10)	0.0001 (6)	-0.0042 (7)	-0.0097 (7)
O4	0.0357 (7)	0.0342 (7)	0.0776 (9)	-0.0038 (5)	0.0003 (6)	0.0007 (6)
O5	0.0388 (7)	0.0394 (7)	0.0692 (9)	0.0071 (6)	0.0068 (6)	0.0055 (6)
N1	0.0663 (14)	0.0417 (11)	0.146 (2)	0.0161 (10)	0.0074 (14)	0.0052 (12)
C1	0.0434 (10)	0.0361 (9)	0.0454 (10)	-0.0060 (8)	0.0105 (8)	-0.0010 (7)
C2	0.0456 (10)	0.0430 (10)	0.0425 (9)	-0.0020 (8)	0.0104 (8)	0.0025 (8)
C3	0.0405 (11)	0.0712 (14)	0.0531 (11)	-0.0039 (10)	0.0073 (9)	0.0057 (10)
C4	0.0482 (12)	0.0840 (16)	0.0469 (11)	-0.0021 (11)	-0.0019 (9)	0.0100 (11)
C5	0.0543 (12)	0.0574 (12)	0.0426 (10)	-0.0041 (10)	0.0072 (9)	0.0073 (9)
C6	0.0456 (10)	0.0383 (9)	0.0449 (10)	-0.0026 (8)	0.0111 (8)	0.0033 (7)
C7	0.0428 (10)	0.0369 (9)	0.0423 (9)	-0.0026 (8)	0.0084 (8)	0.0023 (7)
C8	0.0515 (12)	0.0514 (11)	0.0435 (10)	-0.0046 (9)	0.0051 (8)	0.0039 (8)
C9	0.0468 (12)	0.0589 (13)	0.0579 (12)	-0.0059 (10)	-0.0023 (9)	0.0066 (10)
C10	0.0446 (11)	0.0504 (12)	0.0681 (13)	-0.0026 (9)	0.0120 (10)	0.0083 (10)

C11	0.0500 (11)	0.0398 (10)	0.0562 (11)	-0.0004 (8)	0.0173 (9)	0.0073 (8)
C12	0.0624 (14)	0.0587 (13)	0.0616 (13)	0.0021 (11)	0.0265 (11)	0.0147 (10)
C13	0.0717 (18)	0.091 (2)	0.0900 (19)	0.0077 (15)	0.0449 (16)	0.0277 (15)
C14	0.0535 (15)	0.108 (2)	0.112 (2)	0.0050 (15)	0.0361 (16)	0.0313 (19)
C15	0.0440 (12)	0.0824 (18)	0.0947 (19)	-0.0009 (12)	0.0138 (12)	0.0180 (14)
C16	0.0892 (19)	0.0800 (17)	0.0493 (13)	-0.0006 (14)	0.0238 (12)	0.0166 (11)
C17	0.0734 (16)	0.0784 (16)	0.0419 (11)	-0.0036 (13)	0.0074 (10)	0.0133 (10)
C18	0.0341 (9)	0.0393 (10)	0.0433 (9)	-0.0030 (7)	0.0058 (7)	0.0026 (7)
C19	0.0398 (10)	0.0353 (9)	0.0468 (9)	-0.0033 (8)	0.0058 (7)	-0.0005 (7)
C20	0.0400 (11)	0.0484 (12)	0.0834 (15)	0.0029 (9)	0.0002 (10)	-0.0094 (11)
C21	0.0535 (13)	0.0413 (11)	0.1047 (18)	0.0072 (10)	0.0052 (12)	-0.0174 (12)
C22	0.0525 (12)	0.0392 (10)	0.0766 (14)	-0.0029 (9)	0.0060 (10)	-0.0102 (10)
C23	0.0421 (10)	0.0358 (9)	0.0555 (11)	-0.0051 (8)	0.0078 (8)	-0.0017 (8)
C24	0.0387 (9)	0.0344 (9)	0.0433 (9)	-0.0040 (7)	0.0086 (7)	-0.0004 (7)
C25	0.0418 (10)	0.0394 (10)	0.0590 (11)	-0.0062 (8)	0.0127 (9)	-0.0089 (8)
C26	0.0429 (11)	0.0416 (10)	0.0765 (14)	-0.0016 (9)	0.0163 (10)	-0.0092 (9)
C27	0.0403 (11)	0.0464 (11)	0.0840 (15)	-0.0054 (9)	0.0052 (10)	-0.0069 (11)
C28	0.0440 (11)	0.0393 (11)	0.0772 (14)	-0.0071 (9)	0.0021 (10)	-0.0063 (10)
C30	0.0704 (18)	0.0472 (14)	0.146 (3)	-0.0085 (13)	-0.0075 (17)	-0.0371 (16)
C31	0.0702 (17)	0.0391 (12)	0.122 (2)	-0.0008 (11)	0.0027 (15)	-0.0243 (13)
C35	0.0462 (12)	0.0460 (13)	0.125 (2)	0.0083 (10)	-0.0034 (13)	0.0042 (14)
C36	0.0719 (18)	0.083 (2)	0.118 (2)	0.0415 (16)	0.0091 (16)	0.0200 (17)
C29A	0.048 (5)	0.039 (7)	0.143 (7)	-0.010 (6)	-0.018 (4)	-0.025 (5)
C32A	0.056 (5)	0.065 (4)	0.146 (10)	-0.013 (3)	-0.021 (6)	-0.027 (6)
C33A	0.044 (4)	0.073 (4)	0.186 (12)	-0.007 (3)	-0.026 (5)	-0.008 (7)
C34A	0.042 (4)	0.049 (3)	0.139 (10)	-0.002 (3)	0.012 (4)	-0.009 (4)
C37A	0.137 (11)	0.038 (4)	0.174 (15)	0.001 (5)	0.006 (11)	0.011 (6)
C29B	0.059 (8)	0.036 (10)	0.118 (11)	0.018 (6)	0.005 (7)	-0.011 (6)
C32B	0.050 (5)	0.073 (9)	0.122 (14)	-0.027 (5)	0.007 (8)	-0.034 (9)
C33B	0.043 (5)	0.079 (11)	0.124 (12)	-0.022 (6)	0.009 (7)	-0.040 (9)
C34B	0.025 (5)	0.088 (11)	0.099 (10)	-0.011 (5)	0.013 (5)	-0.040 (8)
C37B	0.133 (8)	0.050 (5)	0.239 (19)	0.009 (5)	0.051 (12)	-0.011 (10)

Geometric parameters (\AA , $^\circ$)

Cu1—Cu1 ⁱ	2.6295 (5)	C20—H20	0.9300
Cu1—O1 ⁱ	1.9570 (13)	C20—C21	1.372 (3)
Cu1—O2	1.9593 (13)	C21—H21	0.9300
Cu1—O3 ⁱ	1.9841 (13)	C21—C22	1.393 (3)
Cu1—O4	1.9590 (13)	C22—C23	1.418 (3)
Cu1—O5	2.1769 (13)	C22—C31	1.439 (3)
O1—C1	1.257 (2)	C23—C24	1.428 (2)
O2—C1	1.260 (2)	C23—C28	1.430 (3)
O3—C18	1.253 (2)	C24—C25	1.436 (3)
O4—C18	1.255 (2)	C25—H25	0.9300
O5—C35	1.215 (3)	C25—C26	1.351 (3)
N1—C35	1.313 (3)	C26—H26	0.9300
N1—C36	1.425 (4)	C26—C27	1.419 (3)

N1—C37A	1.481 (10)	C27—C28	1.414 (3)
N1—C37B	1.498 (11)	C27—C34A	1.369 (14)
C1—C2	1.495 (3)	C27—C34B	1.49 (2)
C2—C3	1.389 (3)	C28—C29A	1.466 (15)
C2—C7	1.407 (3)	C28—C29B	1.35 (3)
C3—H3	0.9300	C30—H30	0.9300
C3—C4	1.373 (3)	C30—H30A	0.9300
C4—H4	0.9300	C30—C31	1.329 (4)
C4—C5	1.392 (3)	C30—C29A	1.34 (2)
C5—C6	1.417 (3)	C30—C29B	1.59 (4)
C5—C17	1.441 (3)	C31—H31	0.9300
C6—C7	1.423 (3)	C35—H35	0.9300
C6—C11	1.429 (3)	C36—H36A	0.9600
C7—C8	1.438 (3)	C36—H36B	0.9600
C8—H8	0.9300	C36—H36C	0.9600
C8—C9	1.349 (3)	C29A—C32A	1.45 (2)
C9—H9	0.9300	C32A—H32A	0.9300
C9—C10	1.431 (3)	C32A—C33A	1.391 (18)
C10—C11	1.410 (3)	C33A—H33A	0.9300
C10—C15	1.398 (3)	C33A—C34A	1.374 (18)
C11—C12	1.418 (3)	C34A—H34A	0.9300
C12—C13	1.401 (3)	C37A—H37A	0.9600
C12—C16	1.421 (4)	C37A—H37B	0.9600
C13—H13	0.9300	C37A—H37C	0.9600
C13—C14	1.365 (4)	C29B—C32B	1.43 (4)
C14—H14	0.9300	C32B—H32B	0.9300
C14—C15	1.382 (4)	C32B—C33B	1.32 (3)
C15—H15	0.9300	C33B—H33B	0.9300
C16—H16	0.9300	C33B—C34B	1.39 (3)
C16—C17	1.318 (4)	C34B—H34B	0.9300
C17—H17	0.9300	C37B—H37D	0.9600
C18—C19	1.504 (2)	C37B—H37E	0.9600
C19—C20	1.394 (3)	C37B—H37F	0.9600
C19—C24	1.419 (3)		
O1 ⁱ —Cu1—Cu1 ⁱ	85.23 (4)	C21—C20—H20	118.7
O1 ⁱ —Cu1—O2	168.37 (6)	C20—C21—H21	119.8
O1 ⁱ —Cu1—O3 ⁱ	87.53 (7)	C20—C21—C22	120.5 (2)
O1 ⁱ —Cu1—O4	91.06 (6)	C22—C21—H21	119.8
O1 ⁱ —Cu1—O5	93.64 (5)	C21—C22—C23	118.57 (19)
O2—Cu1—Cu1 ⁱ	83.18 (4)	C21—C22—C31	122.2 (2)
O2—Cu1—O3 ⁱ	91.29 (7)	C23—C22—C31	119.2 (2)
O2—Cu1—O5	97.96 (5)	C22—C23—C24	121.22 (18)
O3 ⁱ —Cu1—Cu1 ⁱ	79.62 (4)	C22—C23—C28	118.82 (18)
O3 ⁱ —Cu1—O5	91.79 (5)	C24—C23—C28	119.94 (17)
O4—Cu1—Cu1 ⁱ	88.35 (4)	C19—C24—C23	117.85 (16)
O4—Cu1—O2	87.68 (7)	C19—C24—C25	124.61 (16)
O4—Cu1—O3 ⁱ	167.96 (5)	C23—C24—C25	117.54 (17)

O4—Cu1—O5	100.23 (5)	C24—C25—H25	119.1
O5—Cu1—Cu1 ⁱ	171.37 (4)	C26—C25—C24	121.75 (18)
C1—O1—Cu1 ⁱ	121.86 (12)	C26—C25—H25	119.1
C1—O2—Cu1	124.16 (12)	C25—C26—H26	119.1
C18—O3—Cu1 ⁱ	128.45 (12)	C25—C26—C27	121.77 (19)
C18—O4—Cu1	119.31 (12)	C27—C26—H26	119.1
C35—O5—Cu1	117.47 (14)	C26—C27—C34B	119.7 (9)
C35—N1—C36	120.9 (2)	C28—C27—C26	118.53 (19)
C35—N1—C37A	120.6 (11)	C28—C27—C34B	120.7 (10)
C35—N1—C37B	120.2 (10)	C34A—C27—C26	123.1 (6)
C36—N1—C37A	116.3 (9)	C34A—C27—C28	117.9 (6)
C36—N1—C37B	116.7 (8)	C23—C28—C29A	116.8 (8)
O1—C1—O2	125.24 (17)	C27—C28—C23	120.21 (18)
O1—C1—C2	117.02 (17)	C27—C28—C29A	122.9 (8)
O2—C1—C2	117.69 (16)	C29B—C28—C23	125.5 (15)
C3—C2—C1	117.09 (17)	C29B—C28—C27	114.1 (16)
C3—C2—C7	120.03 (17)	C31—C30—H30	119.4
C7—C2—C1	122.85 (17)	C31—C30—H30A	119.3
C2—C3—H3	119.3	C31—C30—C29A	121.2 (6)
C4—C3—C2	121.4 (2)	C31—C30—C29B	121.3 (11)
C4—C3—H3	119.3	C29A—C30—H30	119.4
C3—C4—H4	119.6	C29B—C30—H30A	119.3
C3—C4—C5	120.8 (2)	C22—C31—H31	119.3
C5—C4—H4	119.6	C30—C31—C22	121.5 (2)
C4—C5—C6	118.65 (18)	C30—C31—H31	119.3
C4—C5—C17	122.7 (2)	O5—C35—N1	126.8 (2)
C6—C5—C17	118.6 (2)	O5—C35—H35	116.6
C5—C6—C7	120.60 (18)	N1—C35—H35	116.6
C5—C6—C11	119.45 (17)	N1—C36—H36A	109.5
C7—C6—C11	119.95 (18)	N1—C36—H36B	109.5
C2—C7—C6	118.17 (17)	N1—C36—H36C	109.5
C2—C7—C8	123.96 (17)	H36A—C36—H36B	109.5
C6—C7—C8	117.83 (17)	H36A—C36—H36C	109.5
C7—C8—H8	119.2	H36B—C36—H36C	109.5
C9—C8—C7	121.65 (19)	C30—C29A—C28	122.2 (11)
C9—C8—H8	119.2	C30—C29A—C32A	123.7 (12)
C8—C9—H9	119.2	C32A—C29A—C28	112.6 (15)
C8—C9—C10	121.7 (2)	C29A—C32A—H32A	118.8
C10—C9—H9	119.2	C33A—C32A—C29A	122.3 (12)
C11—C10—C9	118.33 (19)	C33A—C32A—H32A	118.8
C15—C10—C9	122.5 (2)	C32A—C33A—H33A	120.0
C15—C10—C11	119.2 (2)	C34A—C33A—C32A	120.1 (10)
C10—C11—C6	120.39 (18)	C34A—C33A—H33A	120.0
C10—C11—C12	120.24 (19)	C27—C34A—C33A	122.8 (10)
C12—C11—C6	119.4 (2)	C27—C34A—H34A	118.6
C11—C12—C16	119.0 (2)	C33A—C34A—H34A	118.6
C13—C12—C11	118.1 (2)	N1—C37A—H37A	109.5
C13—C12—C16	122.9 (2)	N1—C37A—H37B	109.5

C12—C13—H13	119.3	N1—C37A—H37C	109.5
C14—C13—C12	121.3 (2)	H37A—C37A—H37B	109.5
C14—C13—H13	119.3	H37A—C37A—H37C	109.5
C13—C14—H14	119.5	H37B—C37A—H37C	109.5
C13—C14—C15	121.1 (2)	C28—C29B—C30	113 (2)
C15—C14—H14	119.5	C28—C29B—C32B	123 (3)
C10—C15—H15	120.0	C32B—C29B—C30	116 (2)
C14—C15—C10	120.1 (3)	C29B—C32B—H32B	121.8
C14—C15—H15	120.0	C33B—C32B—C29B	116 (2)
C12—C16—H16	119.0	C33B—C32B—H32B	121.8
C17—C16—C12	122.1 (2)	C32B—C33B—H33B	118.4
C17—C16—H16	119.0	C32B—C33B—C34B	123 (2)
C5—C17—H17	119.3	C34B—C33B—H33B	118.4
C16—C17—C5	121.3 (2)	C27—C34B—H34B	121.9
C16—C17—H17	119.3	C33B—C34B—C27	116.1 (18)
O3—C18—O4	124.08 (17)	C33B—C34B—H34B	121.9
O3—C18—C19	116.05 (16)	N1—C37B—H37D	109.5
O4—C18—C19	119.86 (16)	N1—C37B—H37E	109.5
C20—C19—C18	116.64 (17)	N1—C37B—H37F	109.5
C20—C19—C24	119.19 (17)	H37D—C37B—H37E	109.5
C24—C19—C18	124.11 (16)	H37D—C37B—H37F	109.5
C19—C20—H20	118.7	H37E—C37B—H37F	109.5
C21—C20—C19	122.5 (2)		
Cu1 ⁱ —O1—C1—O2	7.3 (3)	C19—C20—C21—C22	-1.9 (4)
Cu1 ⁱ —O1—C1—C2	-175.04 (12)	C19—C24—C25—C26	-176.85 (19)
Cu1—O2—C1—O1	-6.1 (3)	C20—C19—C24—C23	4.7 (3)
Cu1—O2—C1—C2	176.21 (13)	C20—C19—C24—C25	-175.3 (2)
Cu1 ⁱ —O3—C18—O4	-5.2 (3)	C20—C21—C22—C23	2.9 (4)
Cu1 ⁱ —O3—C18—C19	176.02 (12)	C20—C21—C22—C31	-175.9 (3)
Cu1—O4—C18—O3	5.4 (3)	C21—C22—C23—C24	-0.1 (3)
Cu1—O4—C18—C19	-175.92 (12)	C21—C22—C23—C28	-178.4 (2)
Cu1—O5—C35—N1	-179.5 (3)	C21—C22—C31—C30	175.1 (3)
O1—C1—C2—C3	-38.1 (3)	C22—C23—C24—C19	-3.7 (3)
O1—C1—C2—C7	144.29 (19)	C22—C23—C24—C25	176.31 (19)
O2—C1—C2—C3	139.8 (2)	C22—C23—C28—C27	-178.6 (2)
O2—C1—C2—C7	-37.9 (3)	C22—C23—C28—C29A	1.0 (11)
O3—C18—C19—C20	11.8 (3)	C22—C23—C28—C29B	7 (2)
O3—C18—C19—C24	-171.15 (17)	C23—C22—C31—C30	-3.6 (5)
O4—C18—C19—C20	-167.00 (19)	C23—C24—C25—C26	3.1 (3)
O4—C18—C19—C24	10.1 (3)	C23—C28—C29A—C30	1 (2)
C1—C2—C3—C4	-173.2 (2)	C23—C28—C29A—C32A	166.7 (14)
C1—C2—C7—C6	171.59 (17)	C23—C28—C29B—C30	-10 (3)
C1—C2—C7—C8	-10.8 (3)	C23—C28—C29B—C32B	-157 (3)
C2—C3—C4—C5	1.2 (4)	C24—C19—C20—C21	-2.1 (3)
C2—C7—C8—C9	179.3 (2)	C24—C23—C28—C27	3.0 (3)
C3—C2—C7—C6	-6.0 (3)	C24—C23—C28—C29A	-177.4 (10)
C3—C2—C7—C8	171.7 (2)	C24—C23—C28—C29B	-171 (2)

C3—C4—C5—C6	-5.1 (4)	C24—C25—C26—C27	1.7 (3)
C3—C4—C5—C17	173.2 (2)	C25—C26—C27—C28	-4.1 (4)
C4—C5—C6—C7	3.5 (3)	C25—C26—C27—C34A	168.0 (9)
C4—C5—C6—C11	-177.5 (2)	C25—C26—C27—C34B	-172.2 (13)
C4—C5—C17—C16	-179.4 (3)	C26—C27—C28—C23	1.6 (3)
C5—C6—C7—C2	2.0 (3)	C26—C27—C28—C29A	-177.9 (11)
C5—C6—C7—C8	-175.78 (18)	C26—C27—C28—C29B	176.7 (18)
C5—C6—C11—C10	177.22 (19)	C26—C27—C34A—C33A	-174.9 (9)
C5—C6—C11—C12	-3.6 (3)	C26—C27—C34B—C33B	172.8 (14)
C6—C5—C17—C16	-1.1 (4)	C27—C28—C29A—C30	-179.8 (12)
C6—C7—C8—C9	-3.0 (3)	C27—C28—C29A—C32A	-14 (2)
C6—C11—C12—C13	-179.8 (2)	C27—C28—C29B—C30	175.6 (15)
C6—C11—C12—C16	0.1 (3)	C27—C28—C29B—C32B	28 (4)
C7—C2—C3—C4	4.5 (3)	C28—C23—C24—C19	174.60 (18)
C7—C6—C11—C10	-3.7 (3)	C28—C23—C24—C25	-5.3 (3)
C7—C6—C11—C12	175.38 (19)	C28—C27—C34A—C33A	-2.8 (14)
C7—C8—C9—C10	-0.7 (3)	C28—C27—C34B—C33B	5 (2)
C8—C9—C10—C11	2.3 (3)	C28—C29A—C32A—C33A	12 (2)
C8—C9—C10—C15	-177.7 (2)	C28—C29B—C32B—C33B	-30 (5)
C9—C10—C11—C6	0.0 (3)	C30—C29A—C32A—C33A	177.8 (14)
C9—C10—C11—C12	-179.1 (2)	C30—C29B—C32B—C33B	-176.5 (19)
C9—C10—C15—C14	179.7 (3)	C31—C22—C23—C24	178.8 (2)
C10—C11—C12—C13	-0.6 (3)	C31—C22—C23—C28	0.4 (3)
C10—C11—C12—C16	179.3 (2)	C31—C30—C29A—C28	-4 (2)
C11—C6—C7—C2	-177.02 (17)	C31—C30—C29A—C32A	-168.4 (17)
C11—C6—C7—C8	5.2 (3)	C31—C30—C29B—C28	6 (3)
C11—C10—C15—C14	-0.3 (4)	C31—C30—C29B—C32B	156 (2)
C11—C12—C13—C14	-0.2 (4)	C36—N1—C35—O5	-1.6 (5)
C11—C12—C16—C17	3.1 (4)	C29A—C30—C31—C22	5.4 (13)
C12—C13—C14—C15	0.8 (5)	C29A—C32A—C33A—C34A	-6 (2)
C12—C16—C17—C5	-2.6 (4)	C32A—C33A—C34A—C27	1.2 (17)
C13—C12—C16—C17	-177.0 (3)	C34A—C27—C28—C23	-170.8 (9)
C13—C14—C15—C10	-0.5 (5)	C34A—C27—C28—C29A	9.7 (15)
C15—C10—C11—C6	180.0 (2)	C37A—N1—C35—O5	161.2 (16)
C15—C10—C11—C12	0.9 (3)	C29B—C30—C31—C22	0.4 (17)
C16—C12—C13—C14	179.9 (3)	C29B—C32B—C33B—C34B	17 (3)
C17—C5—C6—C7	-174.9 (2)	C32B—C33B—C34B—C27	-6 (3)
C17—C5—C6—C11	4.2 (3)	C34B—C27—C28—C23	169.7 (12)
C18—C19—C20—C21	175.1 (2)	C34B—C27—C28—C29B	-15 (2)
C18—C19—C24—C23	-172.23 (17)	C37B—N1—C35—O5	-163.9 (17)
C18—C19—C24—C25	7.7 (3)		

Symmetry code: (i) $-x, -y+1, -z$.